University of Stavanger

Faculty of Science and Technology

MASTER'S THESIS

Study program/ Specialization: Master of Science in Mathematics and Physics, Physics Specialization	Spring semester, 2015 Open
Writer: Ejike Obinna Okoye	…… (Writer's signature)
Faculty supervisor: Steinar Evje	
Thesis title: Study Of The 1D Three Phase Liquid, Gas And Cutting Model For Vertical Well Flow	
Credits (ECTS):60	
Key words: Three Phase Navier stoke's model, Compressible flow, Cuttings transport, Matlab Software, New friction term, Injection rates.	Pages: 78 + enclosure: Stavanger,…15/06/2015 Date/year

Study Of The 1D Three Phase Liquid, Gas And Cutting Model For Vertical Well Flow

Ejike Obinna Okoye

June 2015

MASTER THESIS

Institutt for matematikk og naturvitskap
Universitet i Stavanger, Norway

Supervisor: Steinar Evje

Contents

Preface **iii**

Acknowledgement **iv**

1 Introduction **1**

1.1 Background . . . 1

1.1.1 Multiphase flow . . . 1

1.1.2 Drift flux Approach: . . . 2

1.1.3 Two Fluid / Multi-fluid Modeling approach (separation approach) . . . 2

1.1.4 Comparison between Two fluid and Drift flux Approach . . . 3

1.1.5 Flow description . . . 3

1.1.6 Fluid-Solid flow . . . 4

1.1.7 Liquid-Gas flow . . . 5

1.2 Basic Physics On Multiphase Flow . . . 7

1.2.1 Forces in single-component flow . . . 7

1.2.2 Forces acting on a solid particle in suspension . . . 7

1.3 Problem Formulation . . . 8

1.4 Objectives . . . 9

2 Three Phase Navier Stoke Flow Model For Vertical System **11**

2.1 Review Of Various Model Using The Two Fluid Approach . . . 11

2.2 Model Development . . . 14

2.3 Description of Equation . . . 16

2.3.1 Definition of Variables . . . 17

2.4 Closure Models . . . 17

2.4.1 Specific models . . . 17

2.5 Effect of Fanning Friction Factor . . . 30

2.6 A Discrete Approximation-Numerical Scheme . . . 33

2.6.1 Discretization of the continuity equation . . . 33

2.6.2 interior grid cells: j = 2.....,N . . . 34

2.6.3 Discretization of the momentum equation . . . 35

2.7 Intuitive Behaviour Of The Model: . . . 37

3 An Example Of A Base Case Flow Situation **41**

3.1 Specification Of Input Data . . . 41

3.1.1 Description of flow scenario . . . 41

3.1.2 Study of flow simulation result . . . 43

4 Study Of The Injection Rate And Wall Friction Term **56**

4.1 Model Reformulation 56

4.2 Varying of injection rates for the transport system: An example of a base case 56

4.2.1 Effect of cuttings injection rate on pressure and cuttings deposition 58

4.2.2 Effect of liquid injection rates on pressure and cuttings removal 59

4.2.3 Effect of gas injection rate on pressure and cuttings removal 60

4.3 Modified Frictional Term 62

4.3.1 Comparison between the new and old friction term 66

Appendix **71**

List of Figures **71**

List of Tables **73**

References **74**

Preface

This is a Master's thesis in Physics, elaborated at the University of Stavanger in the 2014 Fall and 2015 Spring semesters, as partial accomplishment of the duties due in the Master Course in Mathematics and Physics.

The need to model the challenges that arises from a three phase flow of liquid, gas and cuttings during a drilling operation, has led to several research in this topic. The challenges one would come across while modeling the flow scenario include, but are not limited to, Counter current flow(i.e heavy mud, cuttings that potentially move downwards, gas migrating upwards), transition to single-phase region, sharp gradients(between gas and liquid), expansion of gas at the top due to low pressure there, high fluid-solid interfacial drag force, high pressure gradient due increased fluid injection rate. Therefore, an efficient model which will seek to address the mentioned challenges is necessary.

In this thesis, the use of the numeric Matlab software to generate simulations for the study of the flow scenario shows similar results to other literatures in multiphase flow. The simulation analyses were summarized and recommendations for future work was proposed.

Stavanger, Norway

June 15, 2015

Ejike Obinna Okoye

Acknowledgement

This thesis is the result of my studies at the UiS Institutt for matematikk og naturvitskap. This project could not be realized without the help of a number of people. Therefore my gratitude goes to the following persons.

- Steinar Evje for being my supervisor, for his guidance on this thesis and his effort to see me achieve a good result.
- John Emeka Udegbunam (Assistant professor UiS) and Remi(PhD student UiS) for sharing their ideas in the area of multiphase flow modeling and also for their help in proof reading this work.
- My family and friends for their words of encouragement and prayers.
- Lastly to God Almighty for his grace and love upon my life.

1 Introduction

In this thesis, I will be looking at the transient three phase flow model of Cuttings-liquid-gas in a vertical wellbore. This mathematical model is a three phase viscous Navier stokes model developed to analytically evaluate cuttings transport in a vertical wellbore. The term transient flow model indicates that the flow model describes well conditions that change in time(e.g reduction of bottom hole pressure when injecting nitrogen into a dead well to kick it off for production). An example of what is to be discussed and analysed in this project is a case of a drilling fluid circulated with cuttings plus an inflow of gas at the bottom of the well. This thesis analyses the sensitivity of cuttings transport phenomenon with respect to various parameters using Matlab software. The essence of the use of this software is that it is easy to make simulations and student friendly.

1.1 Background

1.1.1 Multiphase flow

Multiphase flow means that a mixture of gases, liquids and/or solid particles flow together as a mixture, but without being completely dissolved in each other. it is a generalisation of the modelling used where more than two phases are present.

The flow of fluids and particles of a multiphase system has occupied the attention of scientists and engineers for many years. The equation for the motion of multiphase fluids are proposed by the Navier-stokes equations. The major difficulty as said by [3] is the modeling and quantification of turbulence and its influence on mass and momentum transfer. The equations for multiphase flow is considered more primitive in that the correct formulation of the governing equations is still subject to debate.

Multiphase flows can be subdivided into four categories: gas-liquid, gas-solid, liquid-solid and three phase flows. The main idea about the flow system is that one phase acts as the the continuous phase while the other phase is the dispersed phase.

The subject of this thesis as explained earlier is the flow of solid particles and gas in a conveying liquid. But usually in this case, the liquid phase is the continuous phases(carrier phase), while the gas and solid phases (discrete particles or lumps of matter) are the dispersed phases distributed in the continuous phase.

The most rigorous three phase flow modeling approach is the two fluid modeling (separation approach). This approach is considered as a mechanistic model which in general, is the most accurate because they introduce models based on the the detailed physics of each of the different flow patterns [12]. This approach assumes each phase to be considered separately and the model is formulated in three sets of conservation and momentum equations respectively. It however involves considerable difficulties because of the mathematical complications and uncertainties in specifying interfacial interaction.

The difficulties associated with a two phase and three phase model can be significantly reduced by formulating drift flux modeling. It has the advantage of being relatively simple, continuous, and differentiable [12]. The drift flux approach is based on considering two or three phases as a mixture. The drift flux model offers

a single momentum equation for the mixture as a whole in terms of volume averaged velocity of the mixture. This is the fundamental difference between the two fluid approach (separation approach) and the drift flux approach.

In a general compressible formulation,the problem of multi-phase flow in pipes is characterised by strong non-linear coupling between pressure and velocity fields. Solution of the full compressible three-phase problem is required. Such solution could be obtained numerically using iterative schemes. The numerical implementation of an iterative numerical scheme is described by [12]. Such schemes could be applied to obtain solutions for multi-fluid models and drift flux models, see [31] in multiphase flows for oil and gas wells.

1.1.2 Drift flux Approach:

The drift flux model is essentially a flow mixture model in which attention is focused on the relative motion rather than on the motion of the individual phases. the drift flux theory has wide spread application in the dispersion of solid particles in gas,dispersion of solid particles in liquids etc.

The drift flux model is a homogeneous equilibrium flow model. A homogeneous flow theory provides the simplest technique for analyzing two phase(or multiphase) flows. Suitable average properties are determined and the mixture is treated as a pseudofluid that obeys the usual equations of a single component flow. The average properties which are required for a drift flux model are velocity, density and viscosity. These properties are weighted averages and are not necessarily the same as the properties of either phase [1]. The following are the characteristics of a drift flux model:

- Non Newtonian fluid flows
- Homogenous equilibrium flows with averaged properties
- dense, uniformly dispersed little or very little particle size flows with effective mixture properties.

Several formulation for the drift flux model have been developed, see [1] for one dimensional drift-flux equations for mixture flows subjected to body forces.

1.1.3 Two Fluid / Multi-fluid Modeling approach (separation approach)

Separated flow models from the name indicates a side by side interacting fluids, or particles in gas or liquid carrier fluids. This is a heterogeneous flow model which takes into consideration that separate equations of continuity and momentum are written for each phase and these four equations are solved simultaneously, together with rate equations which describe how the phases interact with each other and with the walls of the duct, see [5][pag. 45-49]. Characteristics of a separated flow:

- Phases are identifiable i.e each phase occupies a continuous region with a common interface.
- Two interacting fluid flows where one phase is embedded in the second phase.
- Non uniform, non-equilibrium particle suspension flows

Working with the separated flow model approach, it is important for one to understand the phase properties of the continuous and dispersed phases respectively as well as the flow regime which has to deal with the friction effect involved in the flow system. Navier stokes model for two phase flow using the separation / two fluid approach has been dealt with by several papers and books; [30], [2][pg.292-299], [1][pg.200], [14]

1.1.4 Comparison between Two fluid and Drift flux Approach

Both in the two fluid and drift flux approaches, the continuity equation is written in the same way. i.e for gas and liquid phase, the continuity equation can be written as

$$\frac{\partial}{\partial_t}(\alpha_g \rho_g) + \frac{\partial}{\partial x}(\alpha_g \rho_g v_g) = q_l \tag{1.1}$$

$$\frac{\partial}{\partial_t}(\alpha_l \rho_l) + \frac{\partial}{\partial x}(\alpha_l \rho_l v_l) = q_l \tag{1.2}$$

see [26].

According to [26] the fundamental difference between the two fluid and drift flux approaches is in the formulation of the momentum conservation equation. See table below for comparison.

Two fluid Approach	Drift flux Approach
A set of momentum conservation is written for each phase	momentum conservation equation is written for the volume averaged mixture velocity
The equations contain terms that describe the momentum exchange between phases	Momentum exchange between phases are not specified since it is considered as mixture
Closure relations are required for the momentum exchange terms	additional closure relations is required for the phase velocities
It contains two or three momentum equations which requires more CPU time to calculate	Contains only one momentum equation which requires less CPU time to calculate

Table 1.1: comparison between the two fluid approach and the drift flux approach. see [26]

[26] highlighted a lot of the advantages of the drift flux model in their book.

1.1.5 Flow description

Proper modeling of multiphase flow requires an understanding of the physical system. Two terms that have been used for the classifications of two phase flow are flow pattern and flow regime. When co-current flows of multiple phases occur, the phases take up a variety of configurations, known as flow patterns. A flow pattern indicates the visible distribution or structure of the phases [1]. Unique to two phase and three phase flow, flow

patterns can change in time. The particular flow pattern depends on the conditions of pressure, inflow rates, and channel geometry. In the modeling of flows in a well, knowledge of the flow pattern and flow regimes that would exist in the annulus is essential for defining proper closure models for the friction and interface terms.

The major flow patterns encountered in vertical co-current flow of gas and liquid are; bubbly, slug, churn, and annular. These flow patterns are shown schematically in standard textbooks;[1] and [2] and in the classic works of [17], [18] and [19].

The flow regime in the other hand indicates how the phase distributions affect the physical nature of the system. Hence different flow regimes might indicate the need for different flow models. Two familiar flow regimes are laminar and turbulent flow. Flow regimes are primarily defined by the geometry of the interface.

The question that arises in a three phase flow study which includes a solid phase is, how is the flow pattern and flow regime affected by the transport of the solid phase. First we have to understand basic flow patterns and flow regimes for a gas-liquid vertical flow, solid-liquid vertical flow and gas-solid vertical flow. Based on this understanding, we can redefine closure models that will give a better calculation to obtaining the forces affecting the three phase flow in a vertical system.

In this chapter we will give more insight into the flow conditions experienced in a two phase flow. In two phase flow, flow regimes depend on the type of phase combination(i.e Gas-solid, Gas-liquid, Liquid-solid),flow rates and direction, the conduit shape and size, as well as orientation.

1.1.6 Fluid-Solid flow

The basic idea that will be highlighted here is the flow pattern and flow regimes respectively in a gas-solid interaction system. The introduction of gas at the bottom of a column containing solid particles via a gas distributor can cause solid particle to be fluidized. Several flow patterns/regimes have been observed with increasing fluid inflow rate. These include

- Fixed bed or delayed bubbling
- Bubbling regime
- Slug flow
- Turbulent regime
- Fast fluidization
- Pneumatic Conveying

A pictorial representation of the flow regime adopted from [20] is shown in Figure 1.

Flow pattern in a liquid - solid flow is similar to the above gas-solid flow pattern definition.

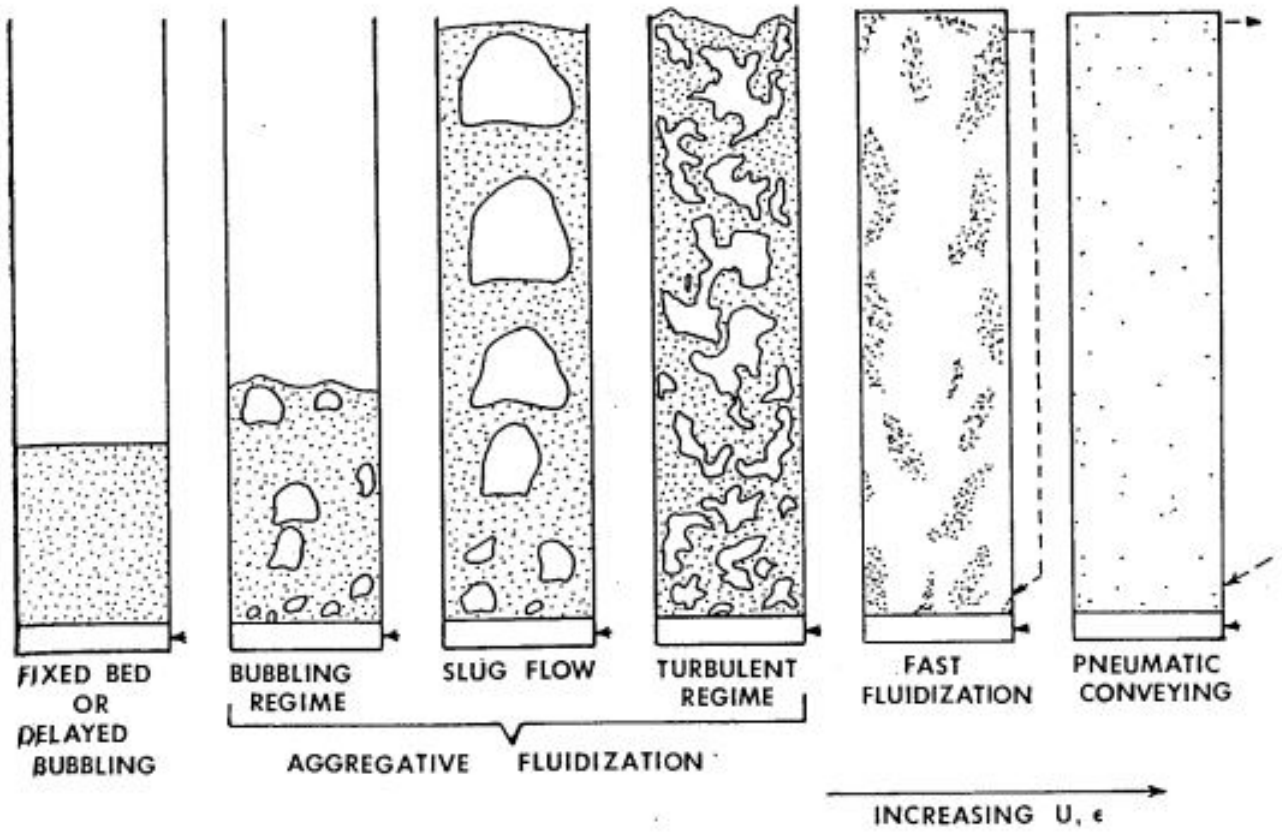

Figure 1.1: Figure showing the flow regime of the Fluid Solid transport in a vertical pipe Adapted from [20]

1.1.7 Liquid-Gas flow

For the liquid-gas flow, The various regimes are defined as follows:

- Bubble flow: The gas-liquid ratio is small. The gas is present as small bubbles, randomly distributed, whose diameters also vary randomly. The bubbles move at different velocities depending upon their respective diameters. The liquid moves up the pipe at a fairly uniform velocity, and except for its density, the gas phase has little effect on the pressure gradient.

- Slug flow: In this regime the gas phase is more pronounced. Although the liquid phase is still continuous, the gas bubbles coalesce and form stable bubbles of approximately the same size and shape, which are nearly the diameter of the pipe. They are separated by slugs of liquid. The bubble velocity is greater than that of the liquid and can be predicted in relation to the velocity of the liquid slug. There is a film of liquid around the gas bubble.

  The liquid velocity is not constant; whereas the liquid slug always moves upward (in the direction of bulk flow), the liquid in the film may move upward, but possibly at a lower velocity, or it may even move downward. These varying liquid velocities not only result in varying wall friction losses, but also result in liquid holdup, which influences flowing density. At higher flow velocities, liquid can even be entrained

in the gas bubbles. Both the gas and liquid phases have significant effects on pressure gradient.

- Churn flow: increased inflow of gas leads to an increase in velocity of the slug-flow bubbles which ultimately leads to a breakdown of these bubbles leading to an unstable regime in which there is an oscillatory motion of the liquid upwards and downwards in the tube.
- Annular flow: The liquid flows on the wall of the tubes as a film and the gas phase flows in the centre.
- Disperse: The tube is completely filled with gas bubbles randomly moving upwards.

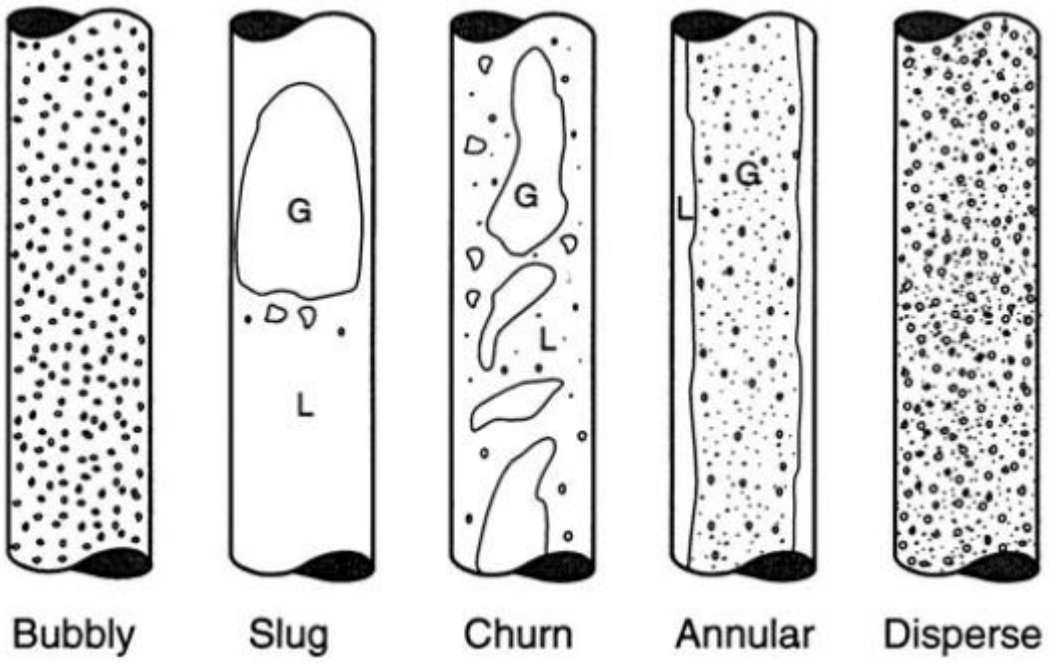

Figure 1.2: Figure showing the flow regime of the Liquid Gas transport in a vertical pipe adapted from [45]

For various flow regimes, mathematical models can be computed to satisfy the flow conditions. Two major divisions of the flow regime are laminar and turbulent flow. These flow regimes depend mainly on the Reynolds number. In fluid mechanics, the Reynolds number (Re) is a dimensionless quantity that is used to help predict similar flow patterns in different fluid flow situations[56]. Knowledge of the Reynolds number can be used to compute for fluid wall friction factor term.

For fluid flow in a vertical pipe, experimental studies shows[21] the following range of Reynolds number for fully developed flow which indicates what flow regime is present.

- laminar flow occurs when $0 < Re_D < 2100$
- transition flow occurs when $2100 < Re_D < 4000$ and
- turbulent flow occurs when $Re_D > 4000$ [22]

The value of the Reynolds number is given as a ratio of the inertia force of the fluid to the viscous force.

$$Re_D = \frac{Inertia force}{Viscous force}, \qquad Re_D = \frac{uD}{\varepsilon},$$

where u is the velocity of the fluid, D is the diameter of the annular duct and ε is the kinematic viscosity.

1.2 Basic Physics On Multiphase Flow

1.2.1 Forces in single-component flow

Whenever a substance is flowing through a conduit, a net force is produced by a concentration gradient. The net force produced by this concentration gradient $\partial\alpha/\partial z$, as long as we remain in a range over which a linear relationship applies [5] is written as;

$$f = \left[\frac{\partial f}{\partial(\partial\alpha/\partial z)}\right]\frac{\partial\alpha}{\partial z} \tag{1.3}$$

Replacing this $\partial\alpha/\partial z$ by a more convenient $\nabla\alpha$, Eq.(1.3) can be written as

$$f = f_{\nabla\alpha}\frac{\partial\alpha}{\partial z} \tag{1.4}$$

For a homogeneous compressible fluids, the concentration α is conveniently measured in terms of mass per unit volume, i.e

$$\alpha = \rho \tag{1.5}$$

The force on a fluid element per unit volume is written as

$$f = -\frac{dp}{dz} = -\frac{\partial p}{\partial\rho}\frac{dp}{dz} \tag{1.6}$$

Hence from Eg.(1.4),

$$f_{\nabla\alpha} = -\frac{\partial p}{\partial\rho} \tag{1.7}$$

The derivative $\partial p/\partial\rho$ should be evaluated along a specified path. for gas and liquid, the isentropic path is usually appropriate. [5]

1.2.2 Forces acting on a solid particle in suspension

- Gravity, F_g, and buoyancy, F_b, are static forces which are due to the properties of the particle and its surrounding fluid only and do not depend on the fluid flow.
- Drag, F_d, and lift, F_L, are hydrodynamic forces incurred by the fluid flow.
- Van der Waals dispersion, F_{van} forces are colloidal forces existing between any neighboring particles.

The forces acting on a suspended solid particle in a fluid can be seen in the figure below

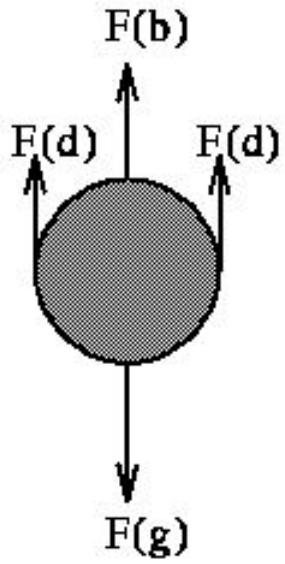

Figure 1.3: Forces acting on a particle settling through a fluid. [53]

A particular question that always arise is how are solid particles transported by fluids through a channel. Well a pictorial view is shown below of various transport process for a solid particle through a channel.

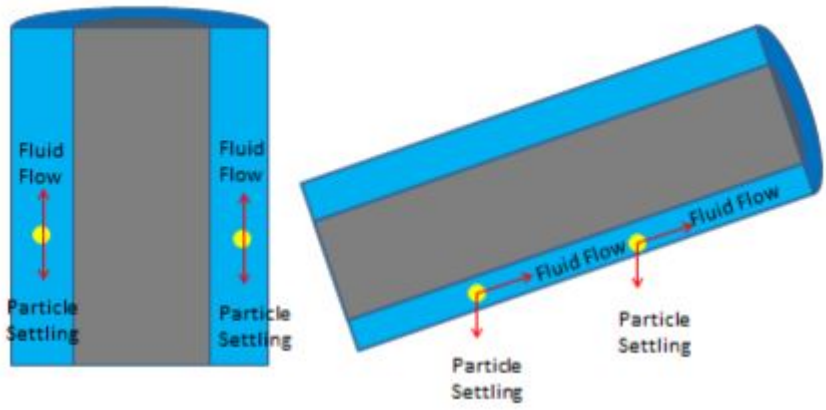

Figure 1.4: Schematic of solid particle transport process in a vertical and horizontal / deviated well [54]

1.3 Problem Formulation

Just like every challenges faced in Multiphase study, we have the following challenges:

- Counter current flow(i.e heavy mud, cuttings that potentially move downwards, gas migrating upwards)
- transition to single-phase region
- sharp gradients(between gas and liguid)
- expansion of gas at the top due to low pressure there.
- frictional force effect on the interacting fluids and cuttings and with the boundary wall.

These problems mentioned above will be observed during the simulation of a base case in section three and proposed solutions in subsequent sections.
It is nice to have a look at various well geometries which can be found in a real drilling situation.

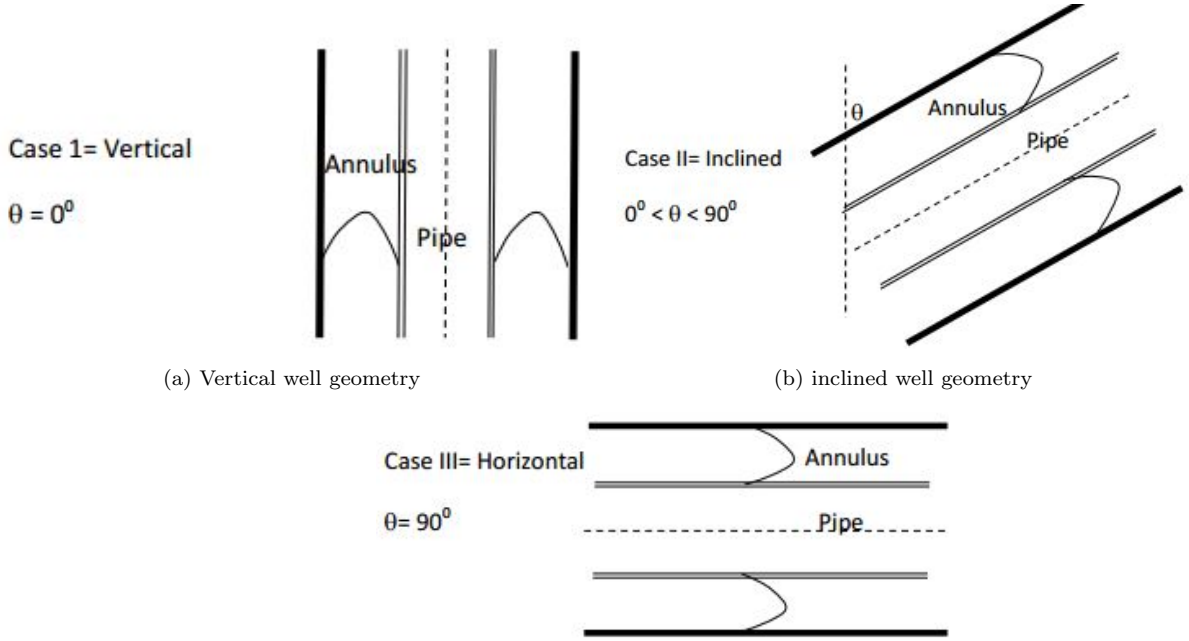

(a) Vertical well geometry

(b) inclined well geometry

(c) Horizontal well geometry

Figure 1.5: Well geometry of various inclinations.[49]

For various geometries, the problem formulation will vary. The problem formulation listed above is with respect to a vertical well geometry.

The introduction of cuttings transport research has led to several studies been carried out and documented. The studies include both experimental and modeling works, which investigated different mechanisms under different operational and fluid-cutting parameters that governs cutting transport.

The model which is going to be discussed in this work might not be an ultimate solution for hole cleaning problem, however it can be used as a tool to understand the physical principles governing the cuttings transport phenomena and how different factors will influence the cuttings transport performance.

1.4 Objectives

The objective of this work is to study certain aspects of a three-phase gas-liquid-cutting model for vertical flow in a well, with this said, The following activity is considered

- Review a general cutting transport model, define closure terms and compute for the well pressure using the method of conservation of volume fraction relation, where basically the idea is to use the error affecting

volume fraction conservation to develop an iterative scheme in which successive pressure corrections are used to adjust densities and velocities until, at convergence, the required conservation is satisfied.

- Simulate the impact of various parameters on cutting transport in a vertical well using Matlab software. The parameters to be used for sensitivity parametric simulation studies were listed in Table 3.1.

  Emphasis is laid on the sensitivity analysis which focuses on the varying volume fraction, velocity profile and the pressure gradient.

- Analysis on the effect of varying injection rates on the pressure curve was done. Here a test of the use of high and low injection rates and its consequences on the well pressure is carried out.

- And lastly, comparison of a modified friction term (which considers the effect of phase density since it is a function of the well pressure with a basic assumption of a laminar flow regime) against the the classic friction term was carried out.

2 Three Phase Navier Stoke Flow Model For Vertical System

2.1 Review Of Various Model Using The Two Fluid Approach

In this section it is wise to review models which have been developed to find an average value for the velocity term, pressure and volume fraction.

A set of one dimensional two fluid model equations based on space and time average presented by [24] was used in the work of [23] " Simulation of the two phase flow in a wellbore using two fluid model". The two phases under consideration were the liquid and gas phase. The 1D continuity equation for both phases is shown below

$$\frac{\partial \langle \alpha_k \rangle \rho_k}{\partial_t} + \frac{\partial}{\partial z}\langle \alpha_k \rangle \rho_k \langle \langle v_k \rangle \rangle = \langle \Gamma_k \rangle \qquad k = 1, 2 \tag{2.1}$$

K represents the two phases liquid and gas respectively and z is the spatial coordinate

Where the first term in the above equation represents the transient term, the second term represents the convective term and the last term on the right represents the change of phase term in this case.

The momentum conservation equation is written as

$$\begin{aligned}\frac{\partial}{\partial t}[\langle \alpha_k \rangle \rho_k \langle \langle v_k \rangle \rangle] + \frac{\partial}{\partial z}[C_{vk}\langle \alpha_k \rangle \rho_k \langle \langle v_k \rangle \rangle^2] = -\langle \alpha_k \rangle \frac{\partial}{\partial z}\langle \langle p_k \rangle \rangle + \frac{\partial}{\partial z}[\langle \alpha_k \rangle \langle \langle \tau_{kzz} + \tau^T_{kzz} \rangle \rangle] \\ -\frac{4\alpha_{kw}\tau_{kw}}{D} - \langle \alpha_k \rangle \rho_k g_z + \langle \Gamma_k \rangle \langle \langle v_{ki} \rangle \rangle + \langle M^d_k \rangle + \langle (p_{ki} - p_k)\frac{\partial \alpha_k}{\partial z} \rangle\end{aligned} \tag{2.2}$$

Starting from the left hand side to the right hand side, the first term is the Transient term, the second is the convective term, the third is the pressure gradient, the fourth is the shear stress term in the direction of the flux, the fifth is the wall friction term, the sixth is the gravitational force(body force), the seventh is the change of phase momentum, the eight is the interfacial momentum transfer and last is the Pressure's difference between fluid and interface.

The above equation is exact, i.e no modelling assumptions has been introduced. Description of the various terms can be seen in the work of [23]. Assumptions were taken to simplify the above momentum equation. In the convective term, C_{vk} is approximated to 1. This has been verified by several authors as indicated in [23] journal. The variation of the shear stress in the flux direction is small due to small velocity variation [23]. This term is set to 0. Moreover, this simplification converts equation(2.2) into an unsteady convective equation with one source term. The interfacial pressure difference $p_{ki} - p_k$ is introduced to ensure the hyperbolicity of the system, see [31]. The interfacial pressure term was discussed by [34] in his thesis work, highlighting several literatures which have dealt with the issue of interfacial pressure. One of the models which expresses remarkable satisfaction is that of CATHARE code which was employed for non stratified flows, [32] and [33]. This model is written as

$$p_k - p_{ik} = \Delta p_{ik} = \gamma \frac{\alpha_g \alpha_l \rho_g \rho_l}{\alpha_g \rho_l + \alpha_l \rho_g}(u_g - u_l)^2 \tag{2.3}$$

where $\gamma = 1.2$ is a factor not necessarily employed by [32] but assumed by [34] in the default expression for

the interfacial pressure difference following the works of [35].

Based on the work of [33],the effects interfacial pressure has on the hyperbolicity of the two-fluid model in the general case of two compressible phases were discussed. Considering a one Dimensional two fluid model for a compressible isentropic flow(process in which entropy remains constant) as shown in equations (1)-(4) of [33], the system can be written in the matrix form defining unknown vector $U = (\alpha_1\rho_1, \alpha_1\rho_1 u_1, \alpha_2\rho_2, \alpha_2\rho_2 u_2)$ as

$$\frac{\partial U}{\partial t} + A(U)\frac{\partial U}{\partial x} = 0 \tag{2.4}$$

and this is said to be strictly hyberbolic if A(U)admits real distinct eigenvalues. Using the abbreviation,

$$\gamma^2 = \frac{c_1^2 c_2^2}{\alpha_1\rho_2 c_2^2 + \alpha_2\rho_1 c_1^2}$$

where $c_1 \& c_2$ are the speed of sound for the two different phases.

Based on the hyperbolicty closure laws, A certain condition for hyperbolicity of the interfacial pressure in equation (2.3), $\Delta p = s u_r^2$ is that

$$s \geq \frac{\alpha_g \alpha_l \rho_g \rho_l}{\alpha_g \rho_l + \alpha_l \rho_g}$$

Implementation of the above model from equation (2.3) using MCBA (mass conservation based algorithm) to obtain solution for the volume fraction and liquid velocity at various time scale can be seen in the work of [23]. Solutions obtained from the model was used to compare with solutions obtained analytically.

A glance at the work of [25] on gas-solid flow in vertical tubes, describes a model adopted from [46] used in the computational study of fully developed gas particle flow in suspension in vertical pipes. [25] focused his work on varying pipe diameters and varying particle sizes. This is to determine the complex manner in which the flow behaviour on a co-current up flow scales up as one increases the pipe diameter. As explained by his work, in circulating fluid beds, the Reynolds number for the gas flow based on the pipe diameter is large and the flow regime will be turbulent at least at low particle concentration. The equation of motions for the momentum balance of gas and solid is represented using cylindrical coordinates. Boundary conditions specifies exchange of pseudo-thermal energy between the particles and wall, where the coefficient of restitution for particle wall collision is specified for the model and also indicated the most important parameter of the gas-solid model besides easily specifiable parameters such as flow rates, particle size and density, tube size etc. was the coefficient of restitution for collision between particles. Two types of collisions where examined for particle interaction; elastic and inelastic collision. For the case of an elastic collision, the value of the coefficient of restitution equals 1 and for the case of an inelastic collision, the values of the coefficient of restitution can vary. Although his experiment focused on elastic collision between particles, in practice most particle collision

are inelastic. A sensitivity analysis of the solid volume fraction for two different values of the coefficient of restitution for particle-particle collision is shown in figure 17 of [25] work. [25] concluded that the effective viscosity of the gas phase can be neglected on certain conditions which he specified but also stated the fact that it begins to become important in a case of dilute suspensions and extremely high gas velocity pneumatic transport.

Discussion about the conservation of the momentum equation using a two fluid approach can be better understood from the book of [6]. According to [6], it can be stated that at a point in the fluid, the stress is written in the usual way $\sigma_J = -p_j\mathbf{I} + \tau_J$ as the sum of a pressure and viscous term. In addition to the fluid stress, at the interface of a solid such as a suspended particle, one may have to consider collisional component σ_C which acts intermittently at isolated points (or small areas) of the entire phase surface. A proposed momentum equation is then written for a phase J where phase change terms are considered.

$$\frac{\partial}{\partial_t}(\alpha_J\langle\rho_J u_J\rangle)+\nabla.(\alpha_k\langle\rho_J u_J u_J\rangle) = \nabla.(\alpha_J\langle\sigma_J\rangle)+\nabla.(\alpha_J\langle\sigma_C\rangle)+\alpha_J\langle\rho_J\rangle\mathbf{g}+\frac{1}{\nu}\int_{S_i}\sigma_J.n_J dS_i-\frac{1}{\nu}\int_{S_i}\rho_J.u_J(u_J-u \tag{2.5}$$

Where the last term accounts for the momentum of phase change. Certain assumptions can be made in neglecting the phase change term. Focusing more on the interfacial integral of σ_J and connecting it with the force that the other phase exerts on the phase J, according to [6] this can be done by combining the interfacial integral with the first term in the right-hand side of equation (2.5),

$$\nabla.(\alpha_J\langle\sigma_J\rangle) + \frac{1}{\nu}\int_{S_i}\sigma_J.n_J dS_i = \alpha_J\nabla.\langle\sigma_J\rangle + \mathbf{F}_J \tag{2.6}$$

Where $\mathbf{F}_J$ is the quantity which is identified with the fluid dynamic force acting on the phase J. Its representation can be seen in equation (8.26)Pg.245 of [6] . Replacing this in equation (2.5), we have

$$\frac{\partial}{\partial_t}(\alpha_J\langle\rho_J u_J\rangle) + \nabla.(\alpha_k\langle\rho_J u_J u_J\rangle) = \alpha_J\nabla.\langle\sigma_J\rangle + \nabla.(\alpha_J\langle\sigma_C\rangle) + \alpha_J\langle\rho_J\rangle\mathbf{g} + \mathbf{F}_J \tag{2.7}$$

The fluid dynamic force constitutes various interaction forces such as the fluid-wall friction force and the inter phase force(force that exists between the interaction of two phases. In a situation where more than two interacting phases are present, the force could be dependent on the third phase or independent). there could be more fluid dynamics type of force.

Similar equations for the momentum conservation of the fluid and particle phase respectively is shown in the book of [1], [26], [27], etc. where the forces present in the flow were highlighted and discussed separately.

Modelling of local forces on a particle suspended in a fluid is discussed extensively in the books of [1] and [6].

According to [6], the effective stress in the particle phase can be partitioned into two parts: a streaming stress, resulting from the fluctuating motion of the particles; and a contact stress, transmitted through direct contact between particles. The contact stress can arise as a result of collisions between particles at low to high particle concentrations. The streaming stress is simply the local average of the phase density and the

difference in phase velocities. The total particle phase stress is expressed as the sum of the rapid flow regime and quasistatic flow regime contributions, [6].

According to phenomenological closures assumption see [8], particle phase stress can be expressed in Newtonian form as

$$\sigma_s = -p_s\mathbf{I} + \mu_s[\nabla u_s + (\nabla u_s)^T] - \frac{2}{3}\mathbf{I}(\nabla . u_s) \tag{2.8}$$

Where particle phase pressure and viscosity are allowed to vary with the particle volume fraction, $p_s = p_s(\alpha_s), \mu_s = \mu_s(\alpha_s)$ and the subscript "s" stands for the solid phase. In a fluid - solid suspension, both of these quantities should vanish as $\alpha_s \to 0$, [6].

Considering the particle - particle interphase term brings a lot of complexity to the modeling of the momentum equation. The importance of particle-particle collisions for rather low volume fractions has been highlighted by [29] and [30]. As particle volume fraction increases particle-particle collisions can have a significant influence on the particle behaviour and the particle phase dynamics. Particle-particle collisions occur due to relative motion between particles that can be caused by several mechanisms, for example Brownian motion of particles, laminar or turbulent fluid shear or particle inertia in turbulent flows [28]. In the work of [29], it was showed that in flows without particle-particle collisions, the mean flow of the particles and fluid is similar, with a relatively small mean slip between the phases. On the other hand, the particle mean velocity can be strongly affected by inter-particle collisions with a flattening of the profile becoming more apparent for the larger Stokes numbers and, therefore, a relatively large mean slip between the phases near the wall.

Other terms that pose difficulties is the viscous stress term. There is not a lot of literature about this term and its effect in the momentum equation of a single or multi-phase flow system. In the book of [1] [Pg.177], the viscous stress term in the momentum equation for the carrier fluid was specified depending upon the the fluid rheology and/or presence of turbulence. An example was looked at for a laminar Newtonian fluid flow, where a mixture(or effective) viscosity was specified μ_m as function of the volume fraction of the solid particle (α_p) or volume fraction of the fluid(α_f) as can be seen below.

$$\vec{\tau} \hat{=} \alpha_f \mu_m (\nabla \vec{u} + \nabla \vec{u}^{tr}) \tag{2.9}$$

Where the viscous stress term includes the change of velocity due to turbulence. In a case of a homogeneous equilibrium model, where same velocity and pressure in both phases are assumed, The viscous stress term can also be written as the sum of the laminar viscous stress and the turbulent viscous stress, see [1] equation 3.112 pg.198.

Other literatures have tried to define a closure term for the viscous stress.

2.2 Model Development

The basis of the three phase model is based on the so called two-fluid model formulation where the gas and liquid phase have separate mass and momentum conservation equations. In particular, the momentum equations involve a non-conservative pressure-related term, a viscous term and external force terms representing

gravity and friction between fluid and wall as well as interphase friction. The one dimensional form of the model is obtained by integrating the flow properties over the cross sectional area of the flow. [1] in his book titled two phase flow (theory and application), gave an in depth discussion on the derivation of Homogeneous flow model for the mass, momentum and energy equation .

The present study is based on the transport equations for a non- isothermal flow and ignoring mass transfer, Hence the mass and momentum equations for the gas, liquid and cuttings phases are presented.

The following assumptions are made for the development of this three phase model

- Non-Isothermal condition: i.e temperature difference is ignored.
- Phase mass transfer is ignored
- The viscous property of the drilling fluid is non-Newtonian and it is time independent. This is referred to as pseudo plastic fluids. The viscosity term which is referred to as the apparent viscosity varies with the shear rate of the fluid and is given as

$$\mu a = \frac{\tau}{\dot{S}} \tag{2.10}$$

  where τ = shear stress and $\dot{S}$= Shear rate

  Time independent non-Newtonian materials are commonly used for solid extractions in pipe flow studies.

- The drilling fluid(carrier fluid)and the gas density respectively will vary along the well. Since the flow is assumed non-isothermal, the densities of the phases are given as a function of only pressure i.e $\rho_i = \rho_i(P)$, $i = l, g, c$
- The density of cuttings is constant
- The fluids are compressible(i.e liquid and gas)
- Equal pressure between cuttings, liquid and gas.
- cross section of the pipe is constant.
- Mass exchange between the phases is neglected.
- Interfacial pressure term is neglected Δp

The continuity and momentum equations for a basic three fluid gas-liquids-cuttings model in 1D is stated below. The continuity equation can be written in an integral form and a differential form.

The differential form of the Continuity equation takes the following form [6]

$$\partial_t(n) + \partial_x(nu_g) = B_g, \tag{2.11}$$

$$\partial_t(m) + \partial_x(mu_l) = B_l, \tag{2.12}$$

$$\partial_t(s) + \partial_x(su_c) = B_c, \tag{2.13}$$

The momentum equation is written in the form

$$\partial_t(nu_g) + \partial_x(nu_g^2) + \alpha_g \partial_x P_g = -f_g u_g - C_1(u_g - u_l) - ng + \partial_x(\varepsilon_g \partial_x u_g) \tag{2.14}$$

$$\partial_t(mu_l) + \partial_x(mu_l^2) + \alpha_l \partial_x P_l = -f_l u_l - C_1(u_g - u_l) + C_2(u_c - u_l) - mg + \partial_x(\varepsilon_l \partial_x u_l) \tag{2.15}$$

$$\partial_t(su_c) + \partial_x(su_c^2) + \alpha_c \partial_x P_c = -f_c u_c - C_2(u_c - u_l) - sg + \partial_x(\varepsilon_c \partial_x u_c) \tag{2.16}$$

Here $n = \alpha_g \rho_g,\ m = \alpha_l \rho_l$ *and* $s = \alpha_c \rho_c$, where the volume fractions satisfies the unity condition

$$\alpha_g + \alpha_l + \alpha_c = 1 \tag{2.17}$$

We can relate the above momentum equation to the momentum equation by [6] with the absence of the added mass term.

For simplicity, we disregard the effects of phase change on the momentum equations. From the momentum equation of the cuttings phase, we may simplify by ignoring the cuttings acceleration term since the liquid phase accelerates the cuttings. In other words for the momentum equation of the cutting phase, equation (2.16) can be replaced by

$$\alpha_c \partial_x P_c = -f_c u_c - C_2(u_c - u_l) - sg + \partial_x(\varepsilon_c \partial_x u_c) \tag{2.18}$$

2.3 Description of Equation

In fluid-solid particle flows in a vertical pipe, several force groups determine the motion of the fluid and particles which can be captured in the momentum equation of the Navier stokes equation for both the continuous and dispersed phases. These force groups are listed in the literatures by [1],[6],[7] and several others. From equations (2.14) - (2.16), we can describe the following terms in the equation.

Here, f_l, f_g and f_c are parameters describing the drag force between the liquid, gas, solid phase and the wall surface, i.e the wall of the annulus duct respectively ,

- $\partial_t(mu_l), \partial_t(nu_g), \partial_t(su_c)$ - represents the transient term which is a variation of the flux term with respect to time.

- $\partial_x(mu_l^2), \partial_x(nu_g^2), \partial_x(su_c^2)$ - represents the convective term.
- $\alpha_m \partial_x P_m, \alpha_n \partial_x P_n, \alpha_c \partial_x P_c$ - represents the pressure gradient
- $f_l u_l, f_g u_g$ and $f_c u_c$ - represents the frictional forces per unit volume between each phase and the wall
- $C_2(u_g - u_l)$ - Interphase friction term between gas and liquid.
- $C_2(u_c - u_l)$ - Interphase friction term between solid and liquid
- mg, ng, sg - represent the buoyancy force for the various phase particles.
- $\partial_x(\varepsilon_g \partial_x u_g), \partial_x(\varepsilon_l \partial_x u_l), \partial_x(\varepsilon_c \partial_x u_c)$ - represent the change in the viscous stress term.

These terms need closure models.

The source term in equations (2.11)-(2.13) is set to zero when we begin simulation because this a closed system. In a closed system, we only have an inlet and outlet situation. The system is not interrupted by external factors such as inflow of fluid from external region.

2.3.1 Definition of Variables

m = liquid mass

n = Gas mass

s = Cuttings mass

ρ_i = phase densities (kg/m^3), liquid→i=l, gas→i=g and cuttings→i=c

u_i = phase velocities (m/s)

B_i = Source term

P = Pressure (Pa)

g = gravity constant, $9.81(m/s^2)$

α_i = phase volume fractions taking value between 0 and 1.

ε_i = phase Viscosity coefficient

μ_i = apparent / dynamic phase viscosities, (Pas)

a_i - phase sound velocities (m/s), $a_l = 1500m/s, a_g = 316.33m/s$

C_1 = interphase drag coefficient between liquid and gas

C_2 = interphase drag coefficient between solid and liquid

fi = wall-phase friction factor

2.4 Closure Models

2.4.1 Specific models

The closure relations needed in the three phase model are for the liquid-wall, gas-wall, cuttings-wall, interfacial shear forces, density-pressure law(since the density of liquid and gas are not constant).

Assumptions:

- Wall friction term: A common model which is based on the prescription of a friction factor, where the shear stress in one dimensional flow is given by

$$\tau = f_i u_i \tag{2.19}$$

Note that the direction of friction is downwards so as to oppose the flow of the fluid and solid particles upwards.

The term u_i stands for the relative velocity between either the liquid and the wall, the gas and the wall, and the cuttings and the wall. In this work, a formulation for the friction factor f has been implemented from the standard definition of friction force acting on a body moving over a surface.

$$f_g = Fn\mu g,\ f_l = Fm\mu,\ f_c = Fs\mu_c, \tag{2.20}$$

where F refers to the fanning friction factor.

- Interfacial forces: examples have been developed to describe the momentum transfer between the continuous and dispersed phase,([1] pg.196, [6] pg.388) , which can be seen in the above momentum equation. one difficulty in evaluating the momentum equation is the inclusion of the solid-solid interaction term. this becomes too difficult to evaluate, this is due to the complexity in the interaction between the solid phase.

$$I_{i,j} = C_i(u_i - u_j) \tag{2.21}$$

Where $C_i = C_1$ and C_2, is represents the momentum transfer coefficient. u_i = velocity of gas and cuttings, and u_j = velocity of the carrier phase (liquid).

The interfacial friction value can be experimentally obtained. The resulting model is highly relevant for various wellbore applications as the important balance between the pressure and external forces and viscous forces are taken into account.

- Density-pressure law (compressible fluids)

Gas and liquid densities needs to be known when solving the proposed multiphase equations since it is a function of the pressure. The compressibility of the fluids is constant in a steady state and may vary in an unsteady state.

$\rho_l = \rho_l(P)$, $\rho_g = \rho_g(P)$, $\rho_c = \rho_c(P)$

Liquid density model:

$$\rho_l = \rho_{l,0} + \frac{P - P_0}{a_l^2} \tag{2.22}$$

Assume water: $\rho_{l,0} = 1000kg/m^3$, $P_0 = 10000$ Pa, $a_l = 1500$ m/s.

Gas density model:

$$\rho_g = \rho_{g,0} + \frac{P_0}{a_g^2}, \quad a_g = 316.33m/s \tag{2.23}$$

Typically, for a gas fluid constant $\rho_{g,0} \geq 0$ is small
The density of cuttings is constant by our assumption.

- Equal pressure

$P_l = P_g = P_c = P$

consequently, pressure is computed as a function of known parameters (m,n,s). First we compute pressure for a two phase liquid-gas flow model, i.e we set $\alpha_c = 0$

From the basic two phase model,

$$\alpha_l + \alpha_g = 1 \tag{2.24}$$

where

$$\alpha_l = \frac{m}{\rho_l(p)}; \qquad \alpha_g = \frac{n}{\rho g(p)} \tag{2.25}$$

from Equation (2.25), we get

$$\frac{m}{\rho_l(p)} + \frac{n}{\rho g(p)} = 1 \tag{2.26}$$

multiplying both sides of the equation by $\rho_l \rho g$, we get

$$\begin{aligned} \rho_l \rho g(\frac{m}{\rho_l(p)} + \frac{n}{\rho g(p)}) &= \rho_l \rho g \\ \rho g m + \rho_l n &= \rho_l \rho g \end{aligned} \tag{2.27}$$

density can be expressed as

$$\rho_l(p) = \rho_{l,0}^T + \frac{p(x,t)}{a_l^2}, \qquad \rho_g(p) = \rho_{g,0}^T + \frac{p(x,t)}{a_g^2} \tag{2.28}$$

$\rho_l(p)$ and $\rho_g(p)$ are the densities of liquid and gas respectively throughout the wellbore.

from Equation (2.28), we insert known parameters to obtain

$$\begin{aligned} n\rho_{l,0}^T + \frac{pn}{a_l^2} + m\rho_{g,0}^T + \frac{pm}{a_g^2} &= (\rho_{l,0}^T + \frac{p}{a_l^2})(\rho_{g,0}^T + \frac{p}{a_g^2}) \\ n\rho_{l,0}^T + \frac{pn}{a_l^2} + m\rho_{g,0}^T + \frac{pm}{a_g^2} &= \rho_{l,0}^T\rho g(s) + \frac{p\rho_{l,0}^T}{a_g^2} + \frac{p\rho_{g,0}^T}{a_l^2} + \frac{p^2}{a_l^2 a_g^2} \end{aligned} \tag{2.29}$$

multiplying through with $a_l^2 a_g^2$, we get

$$p^2 + p[a_l^2(\rho_{l,0}^T - m) + a_g^2(\rho_{g,0}^T - n)] + a_l^2 a_g^2[\rho_{l,0}^T\rho_{g,0} - m\rho_{g,0}^T - n\rho_{l,0}^T] = 0 \tag{2.30}$$

This is a quadratic equation with pressure as the unknown variable. This can be written as

A = 1

B = $a_l^2(\rho_{l,0}^T - m) + a_g^2(\rho_{g,0}^T - n)$

C = $a_l^2 a_g^2[\rho_{l,0}^T\rho_{g,0}^T - m\rho_{g,0}^T - n\rho_{l,0}^T]$

where ρ_l(p) was defined in equation (2.29) to obtain the pressure equation at all coordinate x with respect to time. Similarly, the initial density term is defined at varying time with initial parameters;

$$\rho_{l,0}^T = \rho_{l,0} - \frac{p_0}{a_l^2}, \qquad \rho_{g,0}^T = \rho_{g,0} + \frac{p_0}{a_g^2}$$

We have a simplified quadratic equation were we solve for p

$$F(p) = Ap^2 + Bp + C = 0 \tag{2.31}$$

Next we compute the pressure equation for the three phase model. The cuttings phase is added here. We make the same computation as we had for the two phase model only that we have to include the third phase(i.e cuttings phase).

We use basic assumption as in the two phase model and also include the cuttings phase,

$\rho_C = constant$

$\rho_c(p, x) = \rho_{c,0}$

From the basic three phase model,

$$\begin{aligned} \alpha_l + \alpha_g + \alpha_c &= 1 \\ \alpha_c &= \frac{s}{\rho_c} \end{aligned} \tag{2.32}$$

From equation (2.33), we can obtain

$$\frac{m}{\rho_l(p)} + \frac{n}{\rho_g(p)} + \frac{s}{\rho_c} = 1 \tag{2.33}$$

multiplying both sides of equation(2.34) by $\rho_l\rho_g\rho_c$, we get

$$\begin{aligned} \rho_l\rho_g\rho_c[\frac{m}{\rho_l(p)} + \frac{n}{\rho_g(p)} + \frac{s}{\rho_c(p)}] &= \rho_l\rho_g\rho_c \\ \rho_g\rho_c m + \rho_l\rho_c n + \rho_l\rho_g c &= \rho_l\rho_g\rho_c \end{aligned} \tag{2.34}$$

we insert known parameters to obtain

$$m\rho^T_{c,0}[\rho^T_{g,0} + \frac{p}{a_g^2}] + n\rho^T_{c,0}[\rho^T_{l,0} + \frac{p}{a_l^2}] + s[\rho^T_{l,0} + \frac{p}{a_l^2}][\rho^T_{g,0} + \frac{p}{a_g^2}] = [\rho^T_{l,0} + \frac{p}{a_l^2}][\rho^T_{g,0} + \frac{p}{a_g^2}]\rho^T_{c,0} \tag{2.35}$$

Expanding this equation, we get

$$\begin{aligned} m\rho^T_{g,0}\rho^T_{c,0} + \frac{mp\rho^T_{c,0}}{a_g^2} + n\rho^T_{l,0}\rho^T_{c,0} + \frac{np\rho^T_{c,0}}{a_l^2} + s\rho^T_{l,0}\rho^T_{g,0} + \frac{sp\rho^T_{l,0}}{a_g^2} + \frac{sp\rho^T_{g,0}}{a_l^2} + \frac{sp^2}{a_l^2 a_g^2} = \\ \rho^T_{l,0}\rho^T_{g,0}\rho^T_{c,0} + \frac{p\rho^T_{l,0}\rho^T_{c,0}}{a_g^2} + \frac{p\rho^T_{g,0}\rho^T_{c,0}}{a_l^2} + \frac{p^2\rho^T_{c,0}}{a_l^2 a_g^2} \end{aligned} \tag{2.36}$$

multiplying through with $a_l^2 a_g^2$, we obtain

$$\begin{aligned} p^2(\rho^T_{c,0} - s) + p[\rho^T_{l,0}\rho^T_{c,0}a_l^2 + \rho^T_{g,0}\rho^T_{c,0}a_g^2 - m\rho^T_{c,0}a_l^2 - n\rho^T_{c,0}a_g^2 - s\rho^T_{l,0}a_l^2 - s\rho^T_{g,0}a_g^2] + \\ \rho^T_{l,0}\rho^T_{g,0}\rho^T_{c,0}a_l^2 a_g^2 - m\rho^T_{g,0}\rho^T_{c,0}a_l^2 a_g^2 - n\rho^T_{l,0}\rho^T_{c,0}a_l^2 a_g^2 - s\rho^T_{l,0}\rho^T_{g,0}a_l^2 a_g^2 = 0 \end{aligned} \tag{2.37}$$

Dividing through with $\rho^T_{c,0}$, we get

$$\mathrm{A} = 1 - \frac{s}{\rho^T_{c,0}}$$

$$\mathrm{B} = \rho^T_{l,0}a_l^2 + \rho^T_{g,0}a_g^2 - ma_l^2 - na_g^2 - \frac{s\rho^T_{l,0}a_l^2}{\rho^T_{c,0}} - \frac{s\rho^T_{g,0}a_g^2}{\rho^T_{c,0}}$$

$$\mathrm{C} = \rho^T_{l,0}\rho^T_{g,0}a_l^2a_g^2 - m\rho^T_{g,0}a_l^2a_g^2 - n\rho^T_{l,0}a_l^2a_g^2 - \frac{s\rho^T_{l,0}\rho^T_{g,0}a_l^2a_g^2}{\rho^T_{c,0}}$$

with

$$\rho^T_{c,0} = \rho_{c,0}$$

We obtain a simplified quadratic equation to find the expression for pressure

$$F(p) = AP^2 + BP + C$$

$$P(m,n,s) = \frac{-B \pm \sqrt{B^2 - 4AC}}{2A} \tag{2.38}$$

A 3-D figure showing pressure as a function of the mass of liquid, gas and cuttings respectively is important in understanding the how these various variables in the pressure equation affects the pressure profile. The graph was produced by considering the following values for the respective variables in the equation;

$\rho_{l,0} = 1000$

$\rho_{g,0} = 0.0$

$\rho_l = \rho_{l,0} - (P_0/a_L^2)$

$\rho_c = 2000$

$P_0 = 100000$

$a_l = 1000$ & 1500;

$a_g = 316.33$

Below we shall have a look at the 3-D pressure graph for the various cases.

- varying cutting mass
- effect of liquid sound velocity and the role played by the compressibility $\frac{1}{a_l^2}$ in equation (2.29).

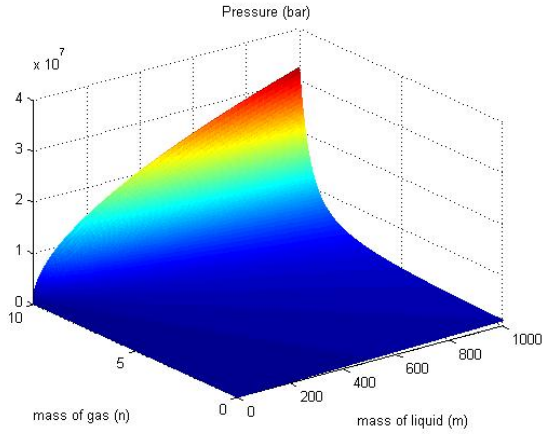

(a) Pressure graph of equ (2.39) as a function m,n and s, with cuttings mass s = 0 kg and liquid commpressibility a_L = 1000 m/s.

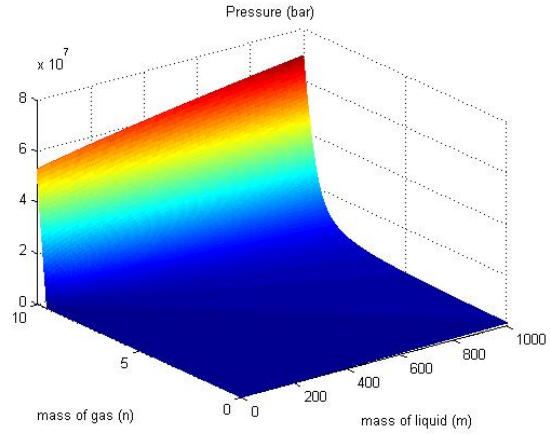

(b) P(m,n,s) of equ (2.39) cuttings mass s = 100 kg and liquid sound velocity a_L = 1000 m/s.

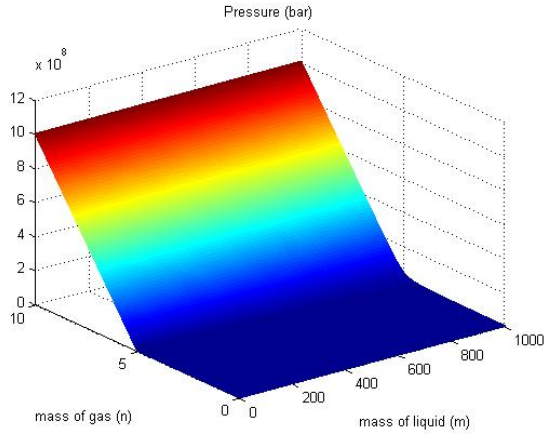

(c) P(m,n,s) of equ (2.39) cuttings mass s = 1000 kg and liquid sound velocity a_L = 1000 m/s.

Figure 2.1: 3-D graph showing pressure as a function of m,n and s at liquid sound velocity a_L = 1000 m/s.

The result obtained from the above 3-D plot shows the rate of pressure increase for varying mass of the cuttings. As seen, negative pressure is not observed and this is due to the fact that the density of gas at all coordinate x is very small $\rho_g \geq 0$.

Furthermore, we also see the effect of liquid compressibility which is tested by increasing the liquid sound velocity a_L to 1500 m/s.

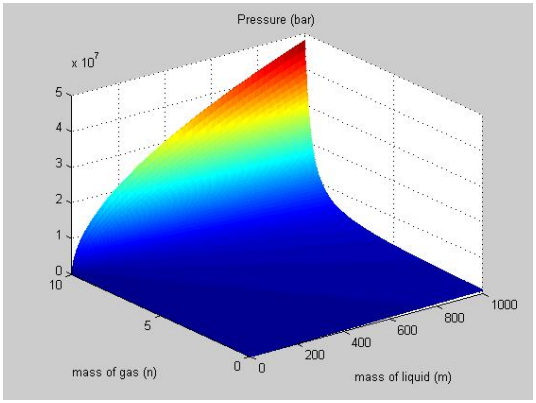

(a) P(m,n,s) of equ (2.39) cuttings mass s = 0 kg and liquid sound velocity a_L = 1500 m/s.

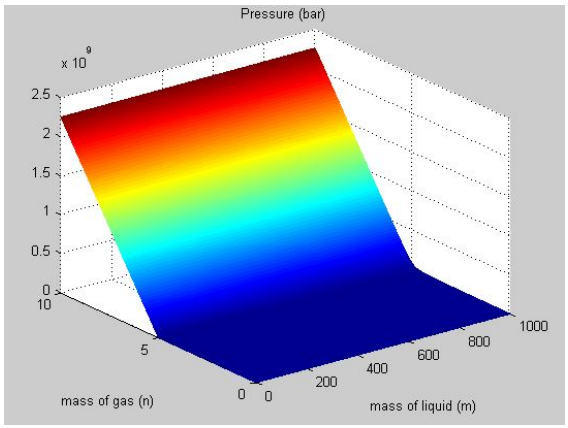

(b) P(m,n,s) of equ (2.39) cuttings mass s = 1000 kg and liquid sound velocity a_L = 1500 m/s.

Figure 2.2: 3-D graph showing pressure as a function of m,n and s at liquid sound velocity a_L = 1500 m/s.

The effect of the increase in the sound velocity for liquid shows an increase on the pressure axis, thereby confirming the theory that increase in a_L, makes the fluid more incompressible, thus increases pressure and lower a_L makes the fluid more compressible, thus lower pressure as seen from Figure 2.1 and 2.2

Remarks: When formulating a cuttings transport model, several assumptions where made. There is need to highlight suggestions which could have been considered in the formulation of the model. Some of these suggestions which are stated below span from several literatures which also dealt with the modeling of cuttings transport either in a vertical, inclined or horizontal well geometry.

Wall friction factor

- In the choice and evaluation of the friction factor, prediction of flow regime transition were not specified.
- As earlier discussed in section one about the work of [23], the wall friction term (f_{kw})can be represented as $f_{kw} = -\frac{4\alpha_{kw}\tau_{kw}}{D}$.
  where τ_{kw} is the phase shear stress which can be written as $\mu_{kw}(\nabla u_{kw})$ and D is the diameter of the pipe.

- Suggestion by [15] for a common model based on the prescription of a friction factor for the liquid-wall, gas-wall friction term and interfacial shear forces. This is given as

$$f_{kw} = \frac{1}{2} f \rho |u_r| u_r \tag{2.39}$$

  where u_r stands for the relative velocity between either the liquid and the wall, the gas and the wall, or the liquid and the gas. [15] in his work, suggested the use of the Hagen -Poiseulle formula which considers a correct prediction of flow regime transition boundaries to define the friction factor between

the gas particles and wall and also for the interfacial friction factors between liquid and gas.

For the gas phase,

$$f_g = \frac{16}{Re_g}, \qquad f_{int} = \frac{16}{Re_{int}}$$

is used in laminar flow or the [42] correlation used for turbulent flow;

$$f_g = 0.046(Re_g)^{-0.2}, \qquad f_{int} = 0.046(Re_{int})^{-0.2}$$

For the liquid phase, the friction factor used, is by [16]. The correlation is given by:

$f_l = \frac{24}{Re_l}$, for laminar flow and $f_l = 0.0262(\alpha_l Re_l)^{-0.139}$ for turbulent flow

The Reynolds numbers Re_g, Re_{int}, Re_l are taken as

$$\begin{aligned} Re_g &= \frac{4A_g u_g \rho_g}{(S_g + S_{int})\mu_g} \\ Re_{int} &= \frac{4A_g |u_g - u_l| \rho_g}{(S_g + S_i)\mu_g} \\ Re_l &= \frac{DU_{sl}\rho_l}{\mu_l} \end{aligned}$$

where $A_g$and A_l are the area occupied by the gas and liquid respectively, the wetted perimeter of the gas and the liquid is S_g and S_l respectively and the interfacial width is S_{int}. [15] noted that the interface Reynolds number Re_{int} is based on the the gas density and the slip velocity between the liquid and gas.

- more suggestion for the friction factor term, [2] defined two phase friction factors in terms of each individual flowing phase and also their mixture, correlating them with the variables that affect them.

$$f_i = -\frac{g_c D}{2\rho_i V_{si}^2}\frac{dP_f}{dX} \tag{2.40}$$

$$f_j = -\frac{g_c D}{2\rho_j V_{sj}^2}\frac{dP_f}{dX} \tag{2.41}$$

where dP_f is the pressure drop in the flow, V_{si}, V_{si} are respectively, the superficial velocities of the i and j phases.

[2] suggested that except in laminar flow, the term dP_f is not predictable from theory and must be determined by measurements. It can be noticed that the viscosity term does not a play any role in determining the friction factor between the phases and the wall surface. Although the choice of the friction

factor definition is arbitrary, [2] suggest that which is based on the superficial velocity and density of one of the phases is simpler to work with.

Interphase term

- The interfacial contributions on a dispersed phase(d) by a continuous phase(c) suggested by [1] can be expressed as

$$I_d = C_{dc}(v_c^{inter} - v_d^{inter}) + (\dot{m}_{dc}v_c^{inter} - \dot{m}_{cd}v_d^{inter})$$

This equation represent the interphase drag and momentum transfer between the continuous phase and dispersed phase. The term C_{dc} represents the interphase drag coefficient. Values for this term can be obtained through experiments.

Also working on the interphase friction was [34], who noted that in a frictionless model, the gas velocity may attain very large values at the end of the tube, where the gas is disappearing. Citing his present work, the gas velocity approached values of several thousand metres per second, leading to stability problems. Also noting similar issue in [35] work,[34] introduced the approach of [35], including an interfacial drag term in the momentum equation:

$$\begin{aligned} F_g^d &= -\Phi\alpha_g\alpha_l\rho_g(u_g - u_l) \\ F_l^d &= \Phi\alpha_g\alpha_l\rho_l(u_g - u_l) \end{aligned}$$

where $F_l^d = -F_g^d$ and $\Phi > 0$ is the friction parameter, adopted from [35], it can be written as;

$$\Phi = Ce^{-k\alpha g}, \quad \Phi = Ce^{-k\alpha_l} \tag{2.42}$$

where $C = 5 \cdot 10^4\ l/s$ and k = 50.

The choices of the values for the parameters were not discussed by [35] but as stated by [34], the above choice of the friction parameter is to impose the interfacial friction in the near-one-phase liquid regions where the gas is expected to dissolve in the liquid. This values are used for separation cases.

The momentum equation also presented in the work of [36] for a gas-solid two phase system which includes the interphase term expresses the interphase momentum transfer coefficient term (β)for a dense region ($\alpha_g < 0.8$). This interphase momentum transfer coefficient is obtained from the well-known Ergun equation:

$$\beta = 150\frac{(1-\alpha_f)^2}{\alpha_f}\frac{\mu_f}{(\phi_s d_p)^2} + 1.75(1-\alpha_f)\frac{\rho_f}{\phi_s d_p}|\bar{u}_f - \bar{u}_s| \tag{2.43}$$

The interphase momentum transfer term is also expressed for a more dilute regime($\alpha_g > 0.8$) from the correlation of [37]

$$\beta = \frac{3}{4}C_d(1-\alpha_f)\frac{\rho_f}{(\phi_s d_p)}|\bar{u}_f - \bar{u}_s|\alpha_f^{-1.65} \tag{2.44}$$

- Particle rotation which accounts for momentum inertia is used in the description of the interaction coefficient term. Consider a Point mass m at a distance r from the axis of rotation. A point mass does not have a moment of inertia around its own axis, but using the "parallel axis theorem" a moment of inertia around a distant axis of rotation is achieved.

  This is given by

$$I = mr^2 \tag{2.45}$$

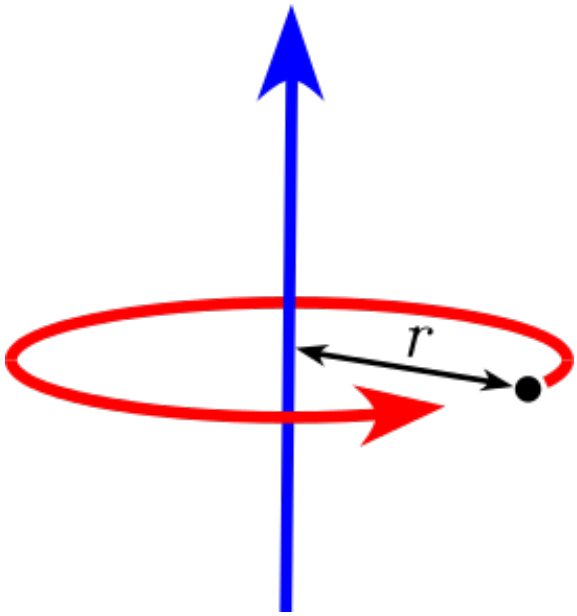

(a) Point mass m at a distance r from the axis of rotation

Figure 2.3: Point mass m at a distance r from the axis of rotation

Two point masses, M and m, with reduced mass ϖ and separated by a distance, x.

This is given by

$$I = \frac{Mm}{M+m}x^2 = \varpi x^2 \tag{2.46}$$

- Effect of drill pipe rotation in directional wells was conducted by several researchers but one experiment done by [10] showed that drill pipe rotation has a significant effect on hole cleaning. His study showed that in most cases the drill string will have both rotary and orbital motion, even when in tension. This

contradicted earlier assumptions by researchers who considered only constraint on the drill pipe to rotate about its own axis, avoiding any orbital motion and concluded that the drill pipe rotation has minimal effect on hole cleaning. According to [10], it is the orbital motion and not the rotation that improves hole cleaning. the orbital motion of the pipe improves the transport of cuttings significantly in two ways: First, the mechanical agitation of the cuttings in an inclined hole sweeps the cuttings resting on the lower side of the hole into the upper side, where the annular velocity is higher. Second, the orbital motion exposes the cuttings under the drill string cyclically to the moving fluid particles

- We have ignored the interaction term between gas and cuttings in the momentum equation $C_3(u_c - u_g)$. The Liquid phase acts as the carrier fluid for the cuttings phase, and therefore the interphase interaction between the gas phase and the cuttings can be neglected since according to the literatures on gas-solid flow, gas-cuttings interaction force can be ignored in a dilute suspension system.[1]

- We also ignored the effect of particle particle interaction influencing individual particle trajectories and random interparticle collisions resulting in brownian-type motion for submicron particles, or particle aggregation. Modelling the particle particle interaction can result in dealing with a complex equation as seen in many literatures one of which is [36]. The modelling equation for a single particle trajectory (Euler-Lagrangian) is discussed by [1] Pg.166-171. Particle-particle interaction due to collision can be modelled in a dilute suspension. Numerous models were postulated, see [3], [4] among others but a simple approach to describe the collision force is given by [1] Pg. 169

$$\vec{F}_{collision} = C_I A_s \frac{\rho}{2}(\vec{v}p - \vec{v})|\vec{v}p - \vec{v}| \tag{2.47}$$

Where C_I is a semi empirical interaction coefficient that depends mainly on the probability of particle collision and intra particle collision impact, A is the area of the particle and ρ is the density of the carrier phase, v_p is the velocity of the moving particle and v is the velocity of the moving fluid.

A work by [44] on the equation for the phase interaction, proposed a model in which the velocity defect in the wake is responsible for the augmentation of turbulence and the work associated with the motion of the particulate phase is responsible for the attenuation of turbulence. They suggested that the turbulence generation is given by

$$G_k = D^2 \rho_c f(l_w)(u^2 - v^2) \tag{2.48}$$

where D is the particle diameter, ρ_c is the density of the carrier phase, $f(l_w)$ is a function of the wake size and u and v are the fluid and particle velocities, respectively. [44] do report, however, good agreement with experimental results.

The momentum equation for a fluid particle mixture has an additional term that accounts for the fluid-dynamic force acting on the fluid per unit volume of mixture and is expressed as [3]

$$f_{d,i} = \frac{1}{V}\Sigma_{i=1}^{N} 3\pi\mu_c D_i f_i (v_i - u_i) \tag{2.49}$$

where N is the number of particles in an averaging volume V, μ_c is the viscosity of the carrier phase, D_i is the particle diameter, f_i is the ratio of the drag coefficient to Stokes drag and v_i and u_i are the particle and fluid velocities, respectively. If the particle size is uniform and f_i is constant, the force term becomes as expressed by [11]

$$f_{d,i} = n3\pi\mu_c D_i f_i(\bar{v}_i - \bar{u}_i) \tag{2.50}$$

where n is the particle number density and the bar over the velocities signifies the number average. For uniform size particles, the number average particle velocity is equal to the volume average, $\langle v_i \rangle = \bar{v}_i$ .The volume average of the carrier fluid velocity is also a reasonable approximation of the number average of the velocity at the particle positions. Finally, the force term can be expressed as

$$f_{d,i} = \beta_v(\langle v_i \rangle - \langle u_i \rangle) \tag{2.51}$$

when the cuttings particles are dense (closely packed),individual particle tracking could be computationally difficult and rather inaccurate. In this case, the fluid and cuttings particle momentum equations are coupled because the swarms of cuttings influence the fluid motion as well.

Viscous stress term

- The viscous stress term was defined for a more laminar flow condition, disregarding the effect of turbulence.
- from the literature of [1], the viscous stress term can be represented with the inclusion of the phase volume fraction, since the volume of each individual phase affects the viscous stress.

2.5 Effect of Fanning Friction Factor

The importance of the fanning friction factor is very relevant to defining the fluid-wall friction term for a two fluid model approach. The Fanning friction factor f depends on the:

- Fluid density
- Velocity
- Viscosity
- Fluid type
- Pipe roughness
- Pipe diameter(ID & OD)

Discussion on the issue of the fanning friction factor has been on for several years. Basically, There are two common friction factors in use, the Darcy friction factor also known as the Darcy–Weisbach friction factor or the Moody friction factor and the Fanning friction factors. Understanding of which friction factor is being described in an equation or chart is important to prevent error in pressure loss, or fluid flow calculation results.

The difference between the two friction factors is that the value of the Darcy friction factor is 4 times that of the Fanning friction factor. They are identical in all other aspect.

The relationship between the two friction factors is represented as:

$$F_D = 4F_f$$

where F_D and F_f represent Darcy and Fanning friction factors respectively. Most literatures I came across laid more emphasis on the use of the Darcy friction factor for analysis on computation of pressure drop and fluid-wall friction interaction [57],[40]. Calculation of the Darcy friction factor using the colebrook equation for turbulent flow condition and the basic formula $f = \frac{64}{Re}$ for laminar flow condition can be seen online. see [59].

Expression of the Fanning friction factor is written as;

$$h_f = 4F_f \left(\frac{L}{D} \frac{V^2}{2g} \right) \tag{2.52}$$

$$h_f = F_d \left(\frac{L}{D} \frac{V^2}{2g} \right) \tag{2.53}$$

where h_f is the head loss due to friction i.e wall friction factor, L is the length of the pipe, D is the pipe diameter, V is the average velocity and g is the acceleration due to gravity.

In calculating the Fanning friction, one has to specify which flow regime is present as said earlier.

For Laminar Flow $Re <\sim 2100$:

In the laminar flow regime, the Darcy Equation may be used to determine the Fanning friction factor:

$$F_d = \frac{64}{Re}, \quad F_f = \frac{F_d}{4}$$

which implies that

$$F_f = \frac{16}{Re}, \qquad Re = \frac{\rho_i u_i D}{\mu_i},$$

This is a dimensionless quantity. The roughness of the pipe is not important in determining the fanning friction for a laminar flow regime as seen in the equation.

For Turbulent Flow regime $Re >\sim 4000$:

For the turbulent flow regime the Colebrook equation is widely accepted for describing the Darcy and Fanning friction factors respectively.

The colebrook equation for calculating the Fanning friction factor is expressed as

$$\frac{1}{\sqrt{F_f}} = -4.0 \log_{10} \left[\frac{\varepsilon/D}{3.7} + \frac{1.26}{Re\sqrt{F_f}} \right] \tag{2.54}$$

where ε is the surface absolute roughness of the pipe and ε/D is referred to as the relative roughness of the pipe.

This equation was developed taking into account experimental results for the flow through both smooth and rough pipe. It is valid only in the turbulent regime for fluid filled pipes. It is widely accepted. Due to the implicit nature of this equation it must be solved iteratively. Where iteration is possible and there are no constraints on computation speed, calculation via the Colebrook equation is appropriate. [57].

According to [40], the friction factor in rough pipes at infinite Reynolds number is calculated from equation (58) by excluding the last part in the brackets.

Other equations which have been developed to solve for explicit calculation of the fanning friction factor can be seen in [40] , [57], [43].

It is also important to note that the colebrook equation can also be used for Laminar flow regime (Reynolds number $Re <\sim 2300$).

Moody plotted the data from the Colebrook equation and this chart which is now known as 'The Moody Chart' or sometimes the Friction Factor Chart, enables a user to plot the Reynolds number and the Relative Roughness of the pipe and to establish a reasonably accurate value of the friction factor for turbulent flow conditions.

Below, a chart of the Moody plot for the fanning friction factor is shown.

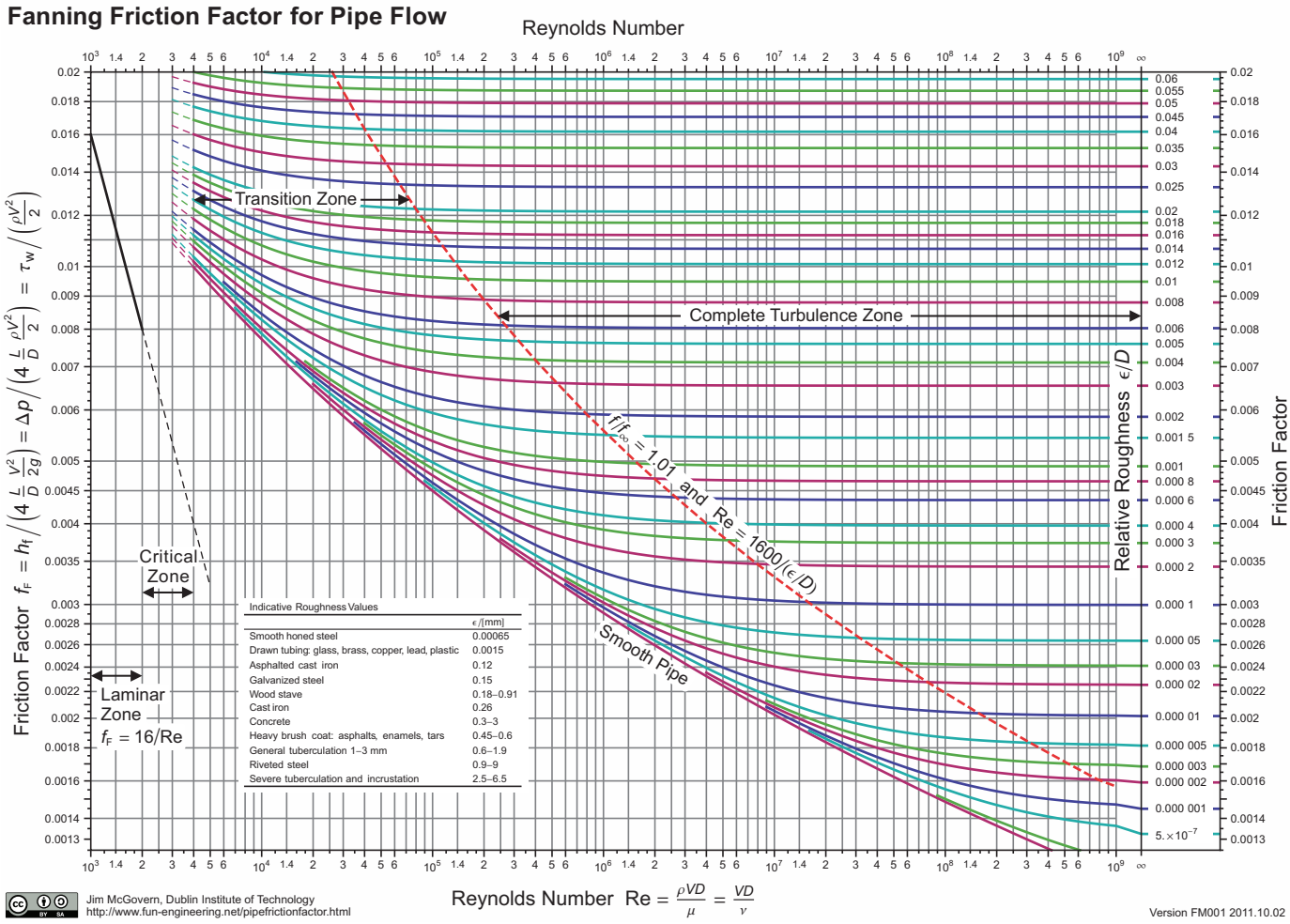

Figure 2.4: Diagram of the Fanning friction factor for pipe flow

2.6 A Discrete Approximation-Numerical Scheme

Consider a discretization of the spatial domain[0,L] into N cells. This gives rise to the grid points $\{x_j\}_{j=1}^{N}$ where x_j is located in the center of the cell $I_j = [x_{j-\frac{1}{2}}, x_{j+\frac{1}{2}}]$. The length of each cell is $\Delta x = x_{j+\frac{1}{2}} - x_{j-\frac{1}{2}}$. All cells are of equal length.

We also consider a discretization of the time interval [0,T] into K steps (of the same length) represented by times $\{t^k\}_{k=1}^{K}$ where the length of each time step is $\Delta = t^{k+1} - t^k$.

2.6.1 Discretization of the continuity equation

A discrete version of the continuity equation (2.11)-(2.13) with an explicit discretization in time then takes the following form:

$$\begin{aligned}
\frac{n_j^{k+1}-n_j^k}{\Delta t}+\frac{1}{\Delta x}(F^k_{j+\frac{1}{2}}-F^k_{j-\frac{1}{2}})=0\\
\frac{m_j^{k+1}-m_j^k}{\Delta t}+\frac{1}{\Delta x}(G^k_{j+\frac{1}{2}}-G^k_{j-\frac{1}{2}})=0\\
\frac{s_j^{k+1}-s_j^k}{\Delta t}+\frac{1}{\Delta x}(H^k_{j+\frac{1}{2}}-H^k_{j-\frac{1}{2}})=0
\end{aligned} \tag{2.55}$$

where the flux term can be approximated as

$$\begin{aligned}
F^k_{j+\frac{1}{2}} &\approx (nu_g)^k_{j+\frac{1}{2}}.\\
G^k_{j+\frac{1}{2}} &\approx (mu_l)^k_{j+\frac{1}{2}}\\
H^k_{j+\frac{1}{2}} &\approx (su_c)^k_{j+\frac{1}{2}}
\end{aligned}$$

Note when we discretize explicitly, we focus on the parameters evaluated at present time t^k. The major advantage of explicit finite difference (discretization) methods is that they are relatively simple and computationally fast. However, the main drawback is that stable solutions are obtained only when

$$0<\frac{\Delta t}{\Delta x}<0.5 \tag{2.56}$$

A semi-explicit variant of equation (2.56) as expressed by [6] can be written as

$$\frac{n_j^{k+1}-n_j^k}{\Delta t}+\frac{1}{\Delta x}n^k_{j+\frac{1}{2}}(u_g^{k+1})_{j+\frac{1}{2}}-n^k_{j-\frac{1}{2}}(u_g^{k+1})_{j-\frac{1}{2}}=0 \tag{2.57}$$

where the importance of the velocities been evaluated at the advanced time t^{k+1} was highlighted by [6]

2.6.2 interior grid cells: j = 2.....,N

For interior part of the domain [0,L] is represented by the cells corresponding to j = 2,.....,N-1. For these cells we employ the discrete approximation of equation (2.56) combined with the discrete approximation of the flux specified.

This gives rise to the following scheme

$$n_j^{k+1} = n_j^k - \lambda(n^k_{j+\frac{1}{2}}(u_g^k)_{j+\frac{1}{2}} - n^k_{j-\frac{1}{2}}(u_g^k)_{j-\frac{1}{2}}); \qquad \lambda = \frac{\Delta t}{\Delta x} \tag{2.58}$$

$$m_j^{k+1} = m_j^k - \lambda(m^k_{j+\frac{1}{2}}(u_l^k)_{j+\frac{1}{2}} - m^k_{j-\frac{1}{2}}(u_l^k)_{j-\frac{1}{2}}) \tag{2.59}$$

$$s_j^{k+1} = s_j^k - \lambda(s^k_{j+\frac{1}{2}}(u_c^k)_{j+\frac{1}{2}} - s^k_{j-\frac{1}{2}}(u_c^k)_{j-\frac{1}{2}}) \tag{2.60}$$

The flux term at the last cell (N) is also computed with same process, keeping in mind that we have assumed gas outside (at surface) and no possibility for liquid entering from top (back flow).

2.6.3 Discretization of the momentum equation

Above we have seen how to discretize the continuity equation, next we show how to discretize the momentum equation. we will illustrate this for the gas phase only. same discretization applies to the other phases.

We start by considering the left hand side of equation (2.14) and since momentum equation is a vector quantity which is centered at half - integer nodes, the control volume or interval over which to carry out the integration is $x_j < x < x_{j+1}$. For the first term, proceeding, we obtain similar to the literature of [6]

$$\frac{1}{\Delta x}\int_{x_j}^{x_{j+1}} dx \frac{(mu)^{k+1} - (mu)^k}{\Delta t} \simeq \frac{(mu)^{k+1}_{j+\frac{1}{2}} - (mu)^k_{j+\frac{1}{2}}}{\Delta t} \tag{2.61}$$

in which $m_{j+\frac{1}{2}} = \alpha_{j+\frac{1}{2}}\rho_{j+\frac{1}{2}}$ and these terms can be evaluated by averaging, e.g.

$$\begin{aligned} \alpha_{j+\frac{1}{2}} &\simeq \frac{1}{2}(\alpha_j + \alpha_{j+1}) \\ \rho_{j+\frac{1}{2}} &\simeq \frac{1}{2}(\rho_j + \alpha_{j+1}) \end{aligned} \tag{2.62}$$

In the convective term,i.e the second term on the left in equation (2.14), we consider that the expression mu^2 should be really understood as $u(mu)$, where the first u is the convection velocity and mu, the momentum density, is the quantity being convected [6]. An explicit or implicit form can be chosen to descritize this term. we will stick to the use of the explicit form.

$$\frac{1}{\Delta t}\int_{t^k}^{t^{k+1}} dt \frac{[(mu)u]_{j+1} - [(mu)u]_j}{\Delta x} \simeq \frac{[[mu]]^k_{j+1}u^k_{j+1} - [[mu]]^k_j u^k_j}{\Delta x} \tag{2.63}$$

Quantities enclosed in double brackets, we refer to as convected quantities.

Usually on grid points, the velocity at cell j is expressed as

$$u_j = \frac{1}{2}(u_{j+\frac{1}{2}} + u_{j-\frac{1}{2}}) \tag{2.64}$$

Also a definition of the nodal mass in terms of the masses of the adjacent cells is stated as:

$$m_j = \frac{1}{2}(m_{j+\frac{1}{2}} + m_{j-\frac{1}{2}}) \tag{2.65}$$

Similarly, since the momentum equation is centered at half integer nodes, we have to develop an estimate for the convected quantity in terms of $[[mu]]_{j+\frac{1}{2}}$. This can be done according to [6] in equation (10.40 page.332)

Therefore the left hand side of the momentum equation becomes

$$\frac{(mu)^{k+1}_{j+\frac{1}{2}} - (mu)^{k}_{j+\frac{1}{2}}}{\Delta t} + \frac{[[mu]]^k_{j+1}u^k_{j+1} - [[mu]]^k_j u^k_j}{\Delta x} \tag{2.66}$$

Elimination of the advanced time m^{k+1} in the time derivative can be done by writing the discretized continuity equation (2.56) at position $j+\frac{1}{2}$ instead of j:

$$\frac{m^{k+1}_{j+\frac{1}{2}} - m^{k}_{j+\frac{1}{2}}}{\Delta t} + \frac{m^k_{j+1}u^k_{j+1} - m^k_j u^k_j}{\Delta x} \tag{2.67}$$

and multiplying this equation by $u^{k+1}_{j+\frac{1}{2}}$ and subtracting from (2.67), we have

$$m^k_{j+\frac{1}{2}} \frac{u^{k+1}_{j+\frac{1}{2}} - u^{k}_{j+\frac{1}{2}}}{\Delta t} + \frac{[[mu]]^k_{j+1}u^k_{j+1} - [[mu]]^k_j u^k_j}{\Delta x} - \frac{m^k_{j+1}u^k_{j+1} - m^k_j u^k_j}{\Delta x} u^{k+1}_{j+\frac{1}{2}} \tag{2.68}$$

The expression (2.69) may be simplified further by approximating the factor $u^{k+1}_{j+\frac{1}{2}}$ by $u^{k}_{j+\frac{1}{2}}$. This can be done without affecting the order of the discretization.

Similarly, the pressure term in the momentum equation can be approximated as

$$\frac{1}{\Delta t \Delta x}\int_{t^k}^{t^{k+1}} dt \int_{x_j}^{x_{j+1}} dx \;\; \alpha \frac{\partial p}{\partial x} \simeq \frac{1}{\Delta t \Delta x}\int_{t^k}^{t^{k+1}} dt \; \alpha_{j+\frac{1}{2}} \int_{x_j}^{x_{j+1}} dx \; \frac{\partial p}{\partial x} \simeq \alpha^k_{j+\frac{1}{2}} \frac{p^k_{j+1} - p^k_j}{\Delta x} \tag{2.69}$$

An explicit discretization was used for the volume fraction and pressure. If we had considered an implicit form, evaluation of the pressure at advanced time step t^{k+1} will lead to a critical situation but is essential in order to update the pressure field.

Referring to [6],it may be necessary to treat part of the source term implicitly, when the associated time scale is very short. This situation arises in this case with the drag terms when interphase momentum transfer is strong. Where the whole momentum equation can be written as:

$$m^k_{j+\frac{1}{2}} \frac{u^{k+1}_{j+\frac{1}{2}} - u^k_{j+\frac{1}{2}}}{\Delta t} + \frac{[[mu]]^k_{j+1} u^k_{j+1} - [[mu]]^k_j u^k_j}{\Delta x} - \frac{m^k_{j+1} u^k_{j+1} - m^k_j u^k_j}{\Delta x} u^k_{j+\frac{1}{2}} + \alpha^k_{j+\frac{1}{2}} \frac{(p^k_{j+1} - p^k_j)}{\Delta x} =$$
$$-F^k_{j+\frac{1}{2}} u^{k+1}_{j+\frac{1}{2}} - (C_1)^k_{j+\frac{1}{2}} ((ug)^{k+1}_{j+\frac{1}{2}} - (u_l)^{k+1}_{j+\frac{1}{2}}) - (ng)^k_{j+\frac{1}{2}} + \frac{\varepsilon^k_{j+\frac{1}{2}} [u^{k+1}_{j+1} - u^{k+1}_j] - \varepsilon^k_{j-\frac{1}{2}} [u^k_j - u^k_{j-1}]}{\Delta x^2} \tag{2.70}$$

A Newton linearization or Picard linearization can be used for the drag terms which often depend non linearly on the velocities. It is important to note that when the interphase drag is strong, the drag parameter C_1 and C_2 will be large.

The above equation just showed the discretization of the momentum equation of the gas phase. Same process is used for the expression of the liquid and cutting phase respectively.

2.7 Intuitive Behaviour Of The Model:

The above model is postulated for the flow of three phases: liquid, gas and cuttings in a vertical well. Well depth is approximated to be 1000 metres and has a diameter of 0.2 metres.

Flow direction is from bottom to top. Pressure at the surface is assumed to be equal to the atmospheric pressure. It is necessary to state that there is no inflow of fluid from the formation into the well and also there is no loss of fluid to the formation.

For various parameters included in the model, we ought to understand the behaviour of this model owing to these parameters. The pressure, density, velocity and flow rate needs to be determined for an effective implementation of this model.

- How does the model behave at initial time zero?
- How is the pressure of the system defined at initial time?
- How is the density of the fluids determined since we assumed compressibility?

In order to obtain a well-posed problem the necessary boundary conditions have to be stated.

Boundary Conditions. We have the following boundary conditions:
We want to implement a situation where we have a specified influx at the bottom $x = 0$ in a domain of length L. This gives rise to the following boundary condition at the bottom:

$$x = 0 : \qquad q_G(x = 0, t) = nu_g,\ q_L(x = 0, t) = mu_l,\ q_C(x = 0, t) = su_c \tag{2.71}$$

and at the top boundary we assume that a known pressure $p^* = P(\rho^*) = P_s(L)$ is specified and known density is also specified $\rho^* = \rho(p^*) = \rho(L)$

$$\begin{aligned} & & P_s(x = L, t) &= 1bar & (2.72)\\ x = L : & & \rho_l(x = L, t) &= \rho_{l,0} + \frac{P_s - P_0}{a_l^2} = 1000, \quad \rho_g(x = L, t) = \rho_{g,0} + \frac{P_s}{a_g^2} = 1, & (2.73)\\ & & \rho_c(x = L, t) &= \rho_c(x = 0, t) & (2.74) \end{aligned}$$

Where
P_0 = atmospheric pressure = $1bar$
P_s = pressure at surface
NB: $P_s = P_0$

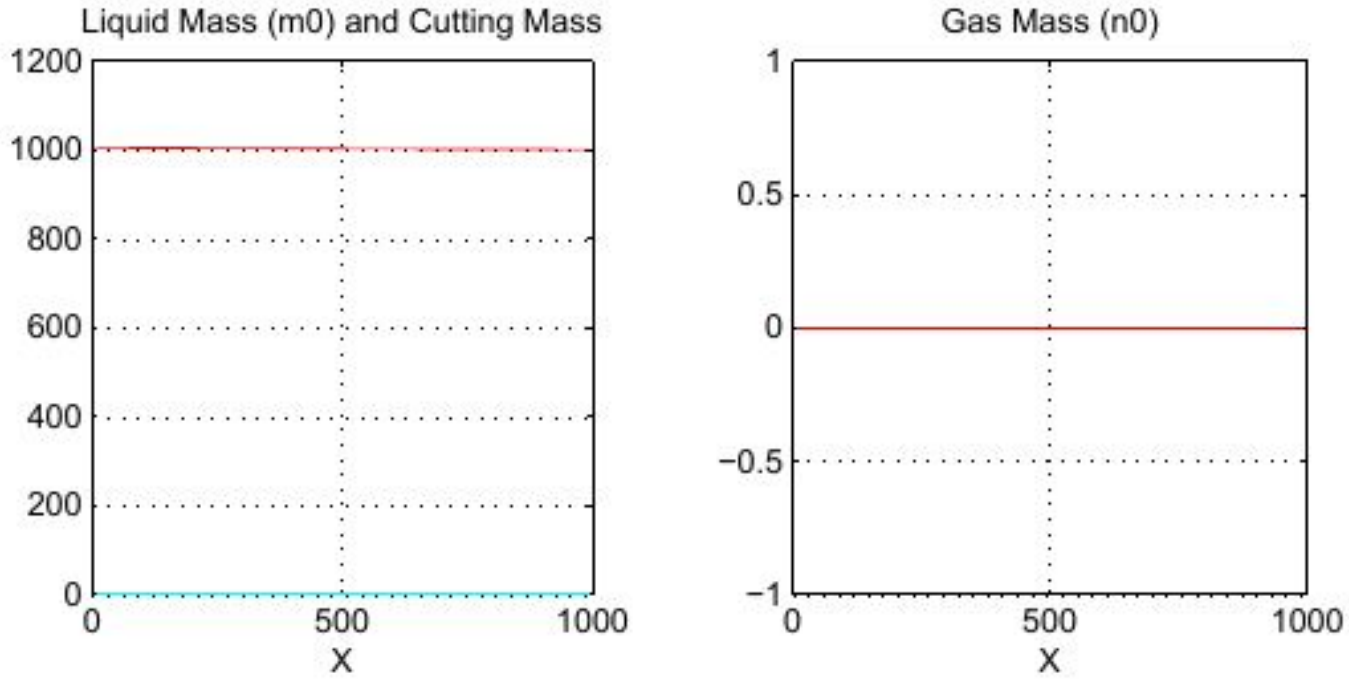

Figure 2.5: Initial state for mass of the various phases

Where the red line indicates the mass of liquid, green line indicates mass of cuttings

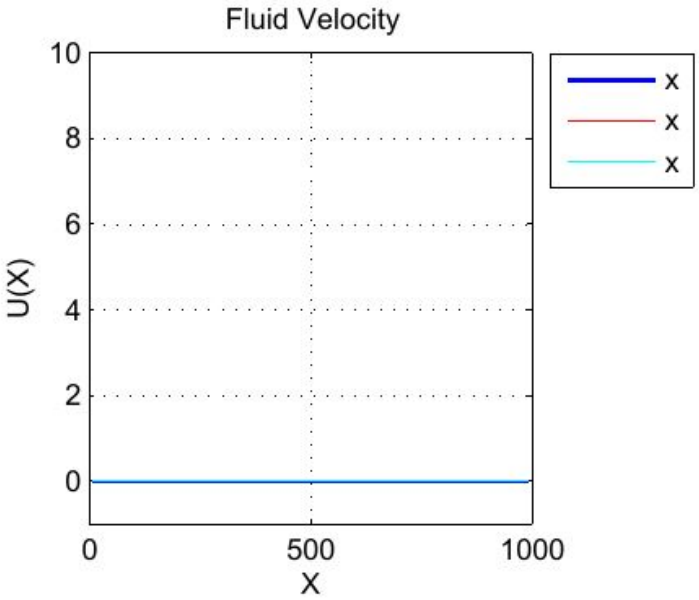

Figure 2.6: Initial state for the fluid velocity of (liquid, Gas and Cuttings)

Where the blue line indicate the velocity of liquid, green line indicates velocity of cuttings and the red line indicates velocity of gas.

Initial data. We must also specify the state$(u, p)(x, t = 0)$ at time zero. A natural choice is to assume that the system is stagnant at initial time. That is

$$u_i(x, t = 0) = 0 \tag{2.75}$$

and from the momentum equation [2.14-2.16] we see that $p(x, t = 0) = p^0$ is given as the solution of

$$\begin{aligned} \alpha_i \partial_x p^0 &= -\alpha_i \rho_i(p^0) g \\ \partial_x p^0 &= -\rho_i(p^0) g \end{aligned} \tag{2.76}$$

introducing the expression for density,

$$\frac{1}{p^0} \partial_x p^0 = \frac{-g}{a_j^2} \tag{2.77}$$

Hence we must solve the ODE equation , we have

$$\frac{-g}{a_j^2} = \frac{1}{p^0} p_x^0, \qquad p^0(L) = p^* = p(\rho^*) = 1 \tag{2.78}$$

where j = liquid, gas.

The solution of this ODE can be found by integration as

$$\int_{p^0(x)}^{p^0(L)} \frac{1}{p^0} dp = \int_x^L \frac{-g}{a_j^2} dx \tag{2.79}$$

$$\ln(p^*) - \ln(p^0(x)) = \frac{-g}{a_j^2}(L - x) \tag{2.80}$$

This gives the solution

$$p^0(x) = p^* \exp(\frac{g}{a_j^2}(L - x)) \qquad x \,\epsilon\, [0, L] \tag{2.81}$$

Similarly, we can also specify the density ρ^0at time zero. using the initial data for the velocity, we can write

$\rho(x, t = 0) = \rho^0$ is given as the solution of

$$\begin{aligned} \alpha_i \partial_x p^0 &= -\alpha_i \rho_i(p^0) g \\ \partial_x p^0 &= -\rho_i(p^0) g \end{aligned} \tag{2.82}$$

introducing the density-pressure law,

$$\frac{1}{\rho^0} \partial_x \rho^0 = \frac{-g}{a_j^2} \tag{2.83}$$

Hence we must solve the ODE equation, , we have

$$\frac{-g}{a_j^2} = \frac{1}{\rho^0} \rho_x^0, \qquad \rho^0(L) = \rho^* = \rho(p^*) \tag{2.84}$$

where j = liquid, gas.

The solution of this ODE can be found as

$$\ln(\rho^*) - \ln(\rho^0(x)) = \frac{-g}{a_j^2}(L - x) \tag{2.85}$$

This gives the solution

$$\rho^0(x) = \rho^* \exp(\frac{g}{a_j^2}(L - x)) \qquad x \,\epsilon\, [0, L] \tag{2.86}$$

$$\rho_g^0(x) = \rho_g^* \exp(\frac{g}{a_g^2}(L - x) \qquad \rho_l^0(x) = \rho_l^* \exp(\frac{g}{a_l^2}(L - x) \qquad \rho_c^0 = constant \tag{2.87}$$

This leads us to express the mass of the phases as a function of their densities

$$m_0 = \alpha_g^0 \rho_g^0(x) \qquad n_0 = \alpha_l^0 \rho_l^0(x) \qquad s_0 = \alpha_c^0 \rho_c^0 \tag{2.88}$$

3 An Example Of A Base Case Flow Situation

3.1 Specification Of Input Data

Below is a table that shows the summary of values of input data and its description.

Descritpion	Units	Input data	Values
Phase volume fraction		α_g	[0,1]
		α_l	[0,1]
		α_c	[0,1)
Density of cuttings	kg/m^3	ρ_c	2000
Atmospheric pressure	Pascal	P_0	10^5
Phase sound velocity	m/s	a_l	1500
		a_g	316.33
Phase viscosity	Pa.s	μ_l	0.15
		μ_g	5×10^{-5}
		μ_c	0.5
Phase viscosity coefficient	Pa.s	ε_{sl}	12×10^7
		ε_{sg}	12×10^6
		ε_{sc}	5×10^7
Fanning friction factor	Dimensionless	K_l	10000
		K_g	10000
		K_c	10000
Interface friction between liquid and gas	kg/m^3s	C_1	500
Interface friction between liquid and cuttings	kg/m^3s	C_2	100
gravity	m/s^2	g	9.81
Area of cross section	m^2	A	$\frac{1}{4}\pi D^2$
Diameter of well Annulus	m	D	0.2
Length of well	m	L	1000

Table 3.1: Model parameters that have been used for the test case

3.1.1 Description of flow scenario

So we consider a real transport situation. A base case of the three phase flow situation using Matlab software to run the test for the given values of various parameters of the model. For an ideal flow situation, a steady state at time zero will occur which refers to a situation where nothing happens, the system is referred to be stagnant. After some time, we start injecting liquid in to the well. The reason for the injection of liquid at an early time, more precisely before the injection of cuttings is that the liquid immediately helps to carry the cuttings up. Gas is injected at a low inflow rate after cuttings is injected. The choice of which type of gas is

injected is not discussed here.

All of these processes has to be captured into the program.

- What is the basis for the choices of the value for the injection rates of the various phases ?
- How much does the information about the injection rate contribute to the model.?
- Is counter current flow observed?
- Do we observe a transition to single phase and at what time?
- What is the effect as we set the phase sound velocity term of liquid and gas flow to 1500 m/s and 316.33 m/s respectively? What happens when the sound velocity is changed. It is important to note that as the speed of sound is reduced, information will be propagated at a lower speed and therefore the pressure and velocity profiles becomes different because it will take a longer time to reach a stationary solution.

All of these questions are basically important in analysing the result of the test. Understanding the flow behaviour of the system will enable one to make appropriate choices of values for the modeling parameters.

Below we have chosen to consider this flow scenario with respect to time. As earlier stated this system is in an unsteady state which means it is time dependent. As regards to our choice below, it is necessary to predict the required minimum flow rate necessary to transport the cuttings to the surface and also still have control over the well pressure. Various literatures have varied the inflow rate at different values in other to obtain a minimum value for effective transport. It is important to note that the choices of flow rates vary with respect to the well inclination. For a horizontal well, the flow rates needed to transport the cuttings maybe higher than in a vertical well.

Generally, inflow rate is obtained by multiplying the mass of the substance, the cross sectional area of the injecting surface and the velocity of the substance. This is mathematically written for the liquid phase as;

$$q_l = nuA \tag{3.1}$$

$$= kgms^{-1}m^2 \tag{3.2}$$

Next we show the flow description at various time step.

- $0 < t < 600$: The system is stagnant
- $600 < t < 5200$: Inflow of liquid at rate $q_l = 700\ kgm^3/s$
- $1000 < t < 5000$: Inflow of cuttings at rate $q_c = 120\ kgm^3/s$
- $2000 < t < 5000$: Inflow of gas at rate $q_g = 20\ kgm^3/s$

- $5000 < t < 9000$: Inflow of gas and cuttings are stopped. The flow rate falls down to zero.
- $5200 < t < 9000$: Inflow of liquid is stopped.

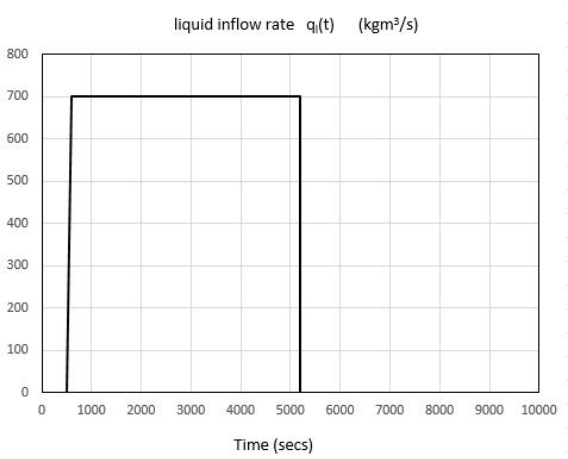

(a) Liquid inflow rate

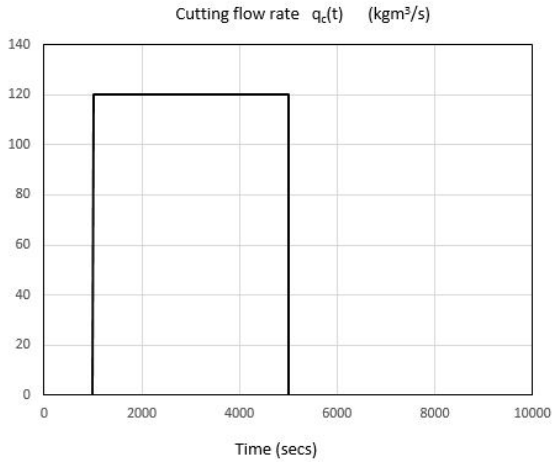

(b) Cuttings inflow rate

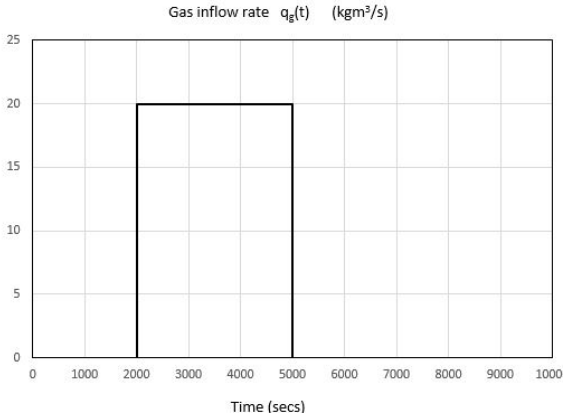

(c) Gas inflow rate

Figure 3.1: Inflow rate of the three phases

The above figure shows the inflow rate of the three different phases independent of one another.

3.1.2 Study of flow simulation result

The system as seen as a control volume, has been solved for a discretized domain of length L. Computing criteria for the test is given below

- Total time of computation was T = 9000 seconds.
- Total number of grid cells, N = 75
- Number of computational time steps, NT = 300

- Plots of the flow rate and pressure terms where recorded at two different wellbore positions;
  N1 = 2 ; position close to the bottom
  N2 = 49; position close to the top

By focusing on the phase volume fractions, velocities and pressure we can understand the entire flow situation and give better suggestion for improvement.

Volume fraction: The following are indicators of the different line colours in the plot.

Green: Liquid phase
Blue: Gas Phase
Sky blue: Cutting phase

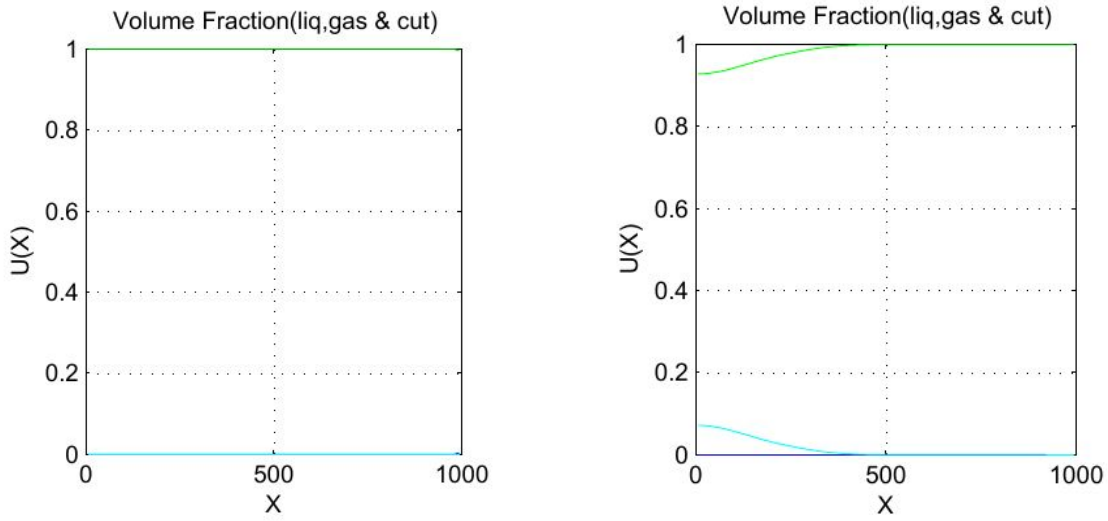

(a) Flow situation at $0 < t < 1000$. Injected liquid occupies the volume of the system, $\alpha_l = 1$

(b) Inflow of cuttings at the bottom of the system at time t = 1000 secs. The cutting begins to occupy the lower part of the well

Figure 3.2: Variation in Volume fractions of all three phases

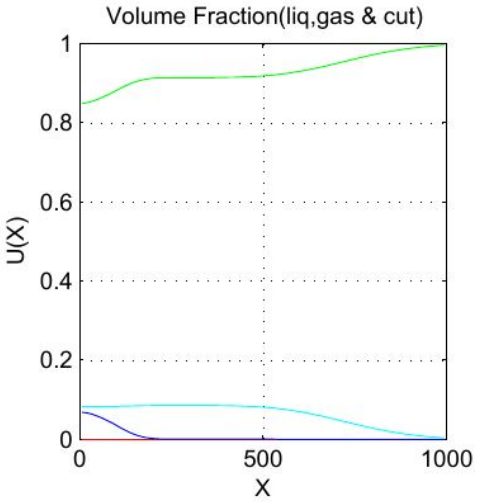

(a) Inflow of gas at time t = 2000 secs. The immediate entry of gas into the system is observed by a gradual decrease in the liquid volume fraction. consequently, a large quantity of cuttings is taking to the surface

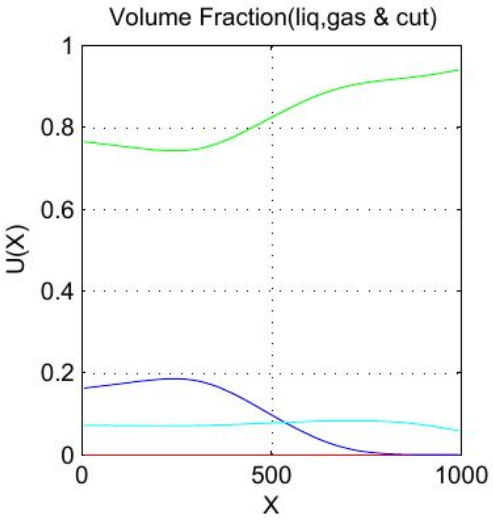

(b) At time t = 3000secs, the volume of gas at the bottom has increased, thus pushing more of the cuttings upwards, which also results in a decrease of the liquid volume at the bottom. Also one point of intersection is seen on gas-solid curve; this point marks the transition to a single phase between the gas and solid flow.

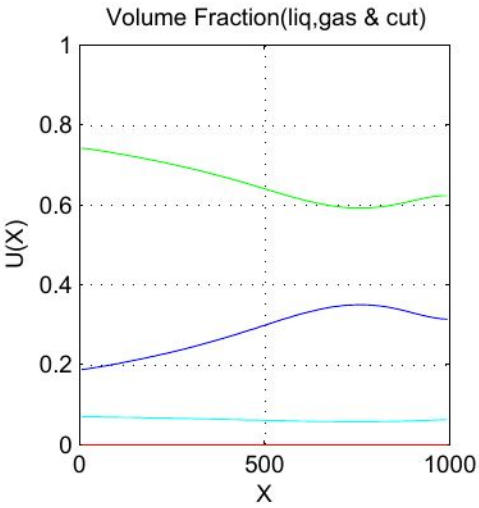

(c) Between time $3500 < t < 4000$ seconds, less dense gas moves to the top as heavy liquid falls to the bottom

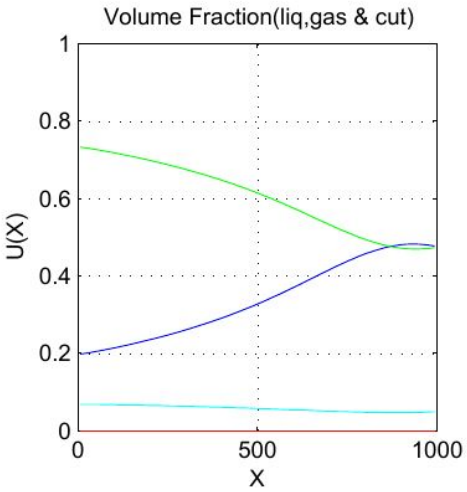

(d) At time t= 4500 sec, we can see the continuation of light gas movement to the top. Here another point of intersection between the gas curve and liquid curve at the surface.

Figure 3.3: Variation in Volume fractions of all three phases

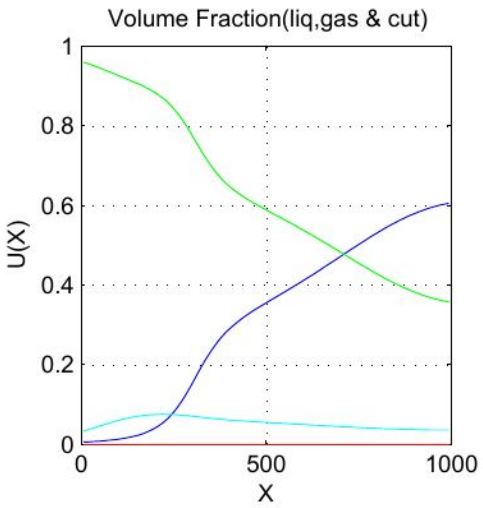

(a) At time t = 5000 secs injection of gas and cuttings is stopped, we observe two intersection points. first between the gas phase and cuttings phase and second between the gas phase and liquid phase.

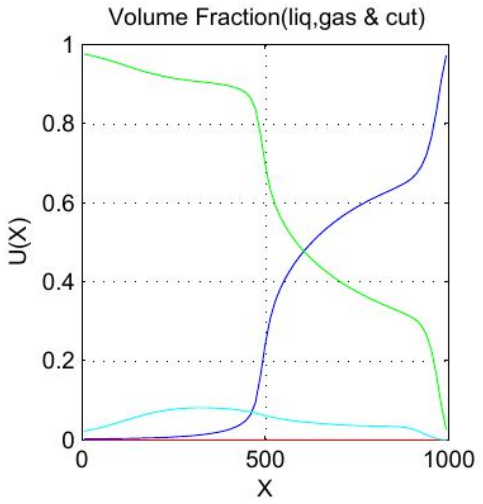

(b) At time t = 5200 secs, liquid injection into the system is stopped. The volume concentration drops down to zero at surface as light gas fraction equals 1 at surface.

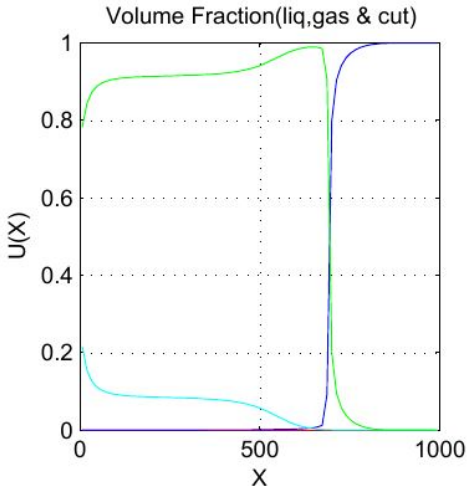

(c) At time t = 9000 secs, a complete transition to single phase is seen.

Figure 3.4: Observation of the behaviour of the curves at the stop of injection and also the transition to single phase

From the plots above, we can make explanations as regards to the liquid, cutting and gas volume fractions respectively.

Liquid:

- At $t = 600$ seconds, the inflow of liquid into the wellbore starts.
- Inflow of cuttings at the bottom, leads to a reduction in the volume fraction of the liquid as more cuttings are packed at the bottom, this due to the compressibility condition of the fluid.

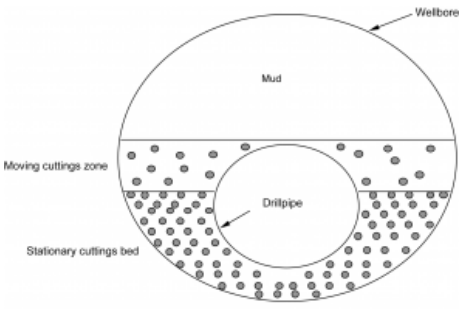

Figure 3.5: Figure showing cutting particles occupying lower side of the wellbore.

- Gas inflow into the system leads to further decrease in the fraction of the fluid at the bottom
- figure 3.3(b) and 3.3(c) shows a steady decrease in the fraction volume of the liquid at the top due to effect of gas migration.
- figure 3.4(c) shows a transition to single phase between the liquid phase and the gas phase.

Cuttings:

- cuttings volume fraction initially set at zero at $0 < t < 1000$.
- Influx of cuttings at the bottom after time $t > 1000$ seconds.
- we have a gradual build up of cuttings concentration from the bottom all the way up to the surface of the wellbore. This is due to the interfacial liquid-cutting term.
- from figure 3.3(a) and 3.3(b) gas build up at the bottom, leads to push in the cutting volume upwards towards the surface . This process continues repeatedly until circulation is stopped.
- when circulation is stopped, we can see a gradual decrease of the cuttings fraction at the top. Heavy cuttings sink to the bottom as seen in figure 3.4(a), 3.4(b) and 3.4(c).

Gas:

- Gas volume fraction initially set to zero at $t > 2000$ seconds
- Injection of gas at the bottom after T = 2000s, leads to a gradual expansion to the surface as seen in figure 3.3(a) and 3.3(b).
- gradual migration of gas to the surface due to density and diffusive property of gas.
- At t = 5000 seconds, gas injection is stopped. the gas volume fraction goes to zero at the bottom and gradually rises to the surface.
- The viscosity term also plays a major role in the migration of gas in the wellbore. Due to the fact that the viscosity of gas is less than that of drilling fluid and the cuttings, the mobility of gas is higher than

that of the drilling fluid, therefore leading to an increase in the velocity of gas.

Below we see a pictorial view of the cuttings-gas volume fraction variation.

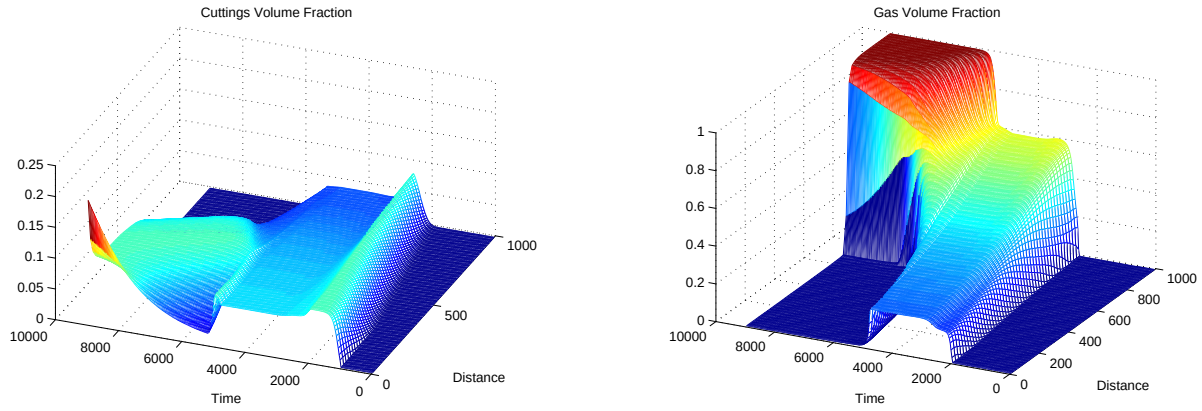

(a) number of descretized cell = 75, Final time = 9000s

(b) number of descretized cell = 75, Final time = 9000s

Figure 3.6: Volume fractions

Phase Velocity Analysis:

The superficial velocity term was used to express the speed of the fluids in the base case flow situation. When expressing the flow rate of a fluid in a system, the velocity of the fluid is calculated as if the system is empty i.e disturbances are ignored. This velocity is referred to as the superficial velocity.

The superficial velocity term can be calculated from the knowledge of the volume fraction. Using the concept of volume fraction, the dependence between the advection velocity and the superficial velocity can be expressed as (for one-dimensional flow):

$$u_s = \alpha u \tag{3.3}$$

Expanding the superficial velocity by taking a look at Equation (3.1), making the velocity the subject of formula, we have

$$u = \frac{q}{nA} \tag{3.4}$$

$$u_s = \alpha \frac{q}{\alpha \rho A} \tag{3.5}$$

$$= \frac{q}{\rho A} \tag{3.6}$$

$$\tag{3.7}$$

Where the superficial velocity is dependent on the flow rate, density and cross sectional area of the flow channel.

$$u_{sl} = \frac{q_l}{\rho_l A}, \quad u_{sg} = \frac{qg}{\rho_g A}, \quad u_{sc} = \frac{qc}{\rho_c A} \tag{3.8}$$

We can discuss the results of the fluid velocities(m/s) obtained in the base case situation from the plots below.

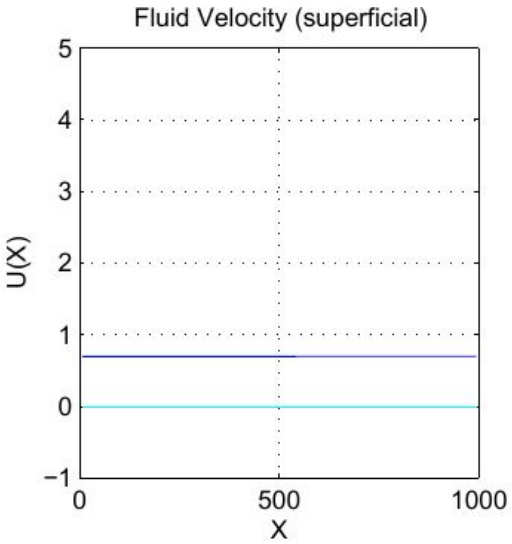

(a) Uniform liquid velocity at time t = 600 sec, time of liquid injection.

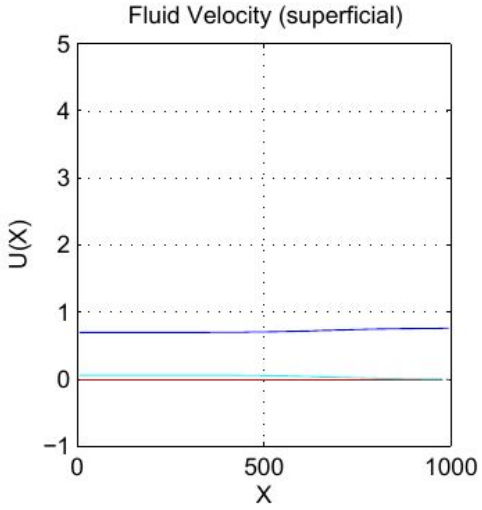

(b) Injection of cutting at time t=1000 sec, shows a low cuttings velocity which means that the speed which the cuttings travels with is very minimal

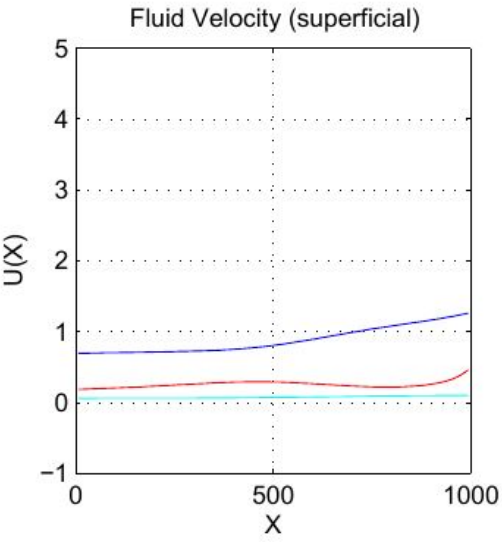

(c) Between the time $2000 < t < 3000$sec, the injection of gas into the system shows a nearly uniform speed of gas flow

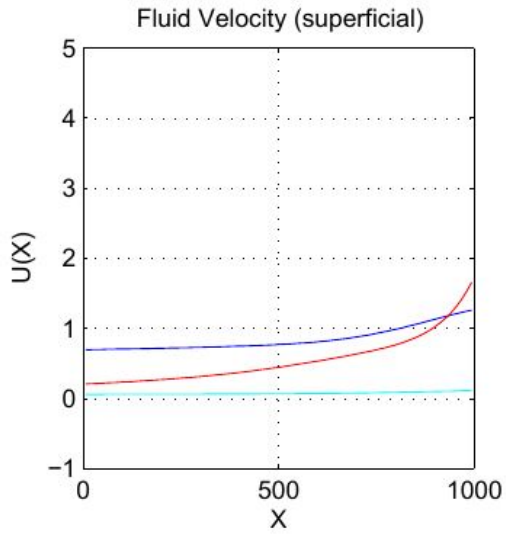

(d) At time t = 4000 secs, the gas velocity curve intersects the liquid velocity curve at the surface. This shows how much time the gas had to travel before it can exceed the liquid velocity

Figure 3.7: Figure showing the Velocity Profile of the three different phases

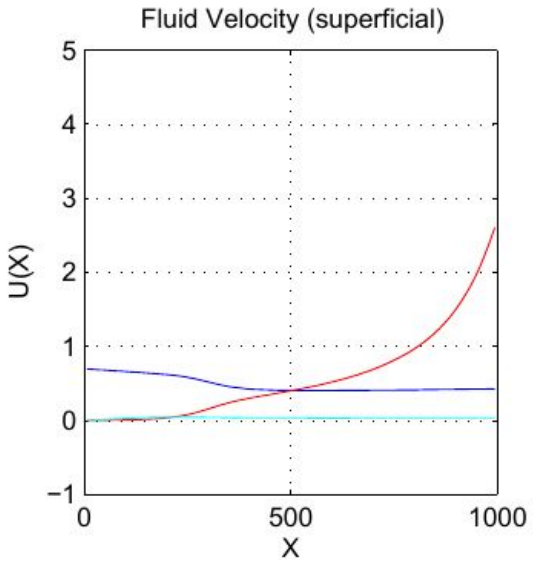

(a) At the time which the gas and cutting injection into the system is stopped, the velocity of the gas phase increases at the surface resulting in a reduced lquid speed and goes to zero at the bottom

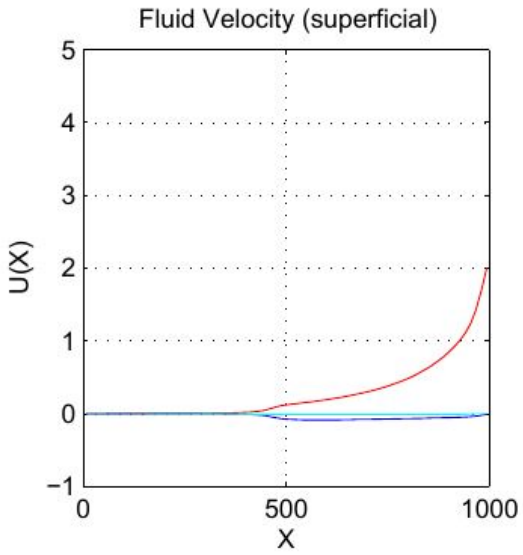

(b) At the time which the liquid injection stops, a negative velocity at the surface is observed which indicates the downward movement of the liquid.

Figure 3.8: Velocity profile after the stop of injection

Observation:

Liquid:

- Uniform velocity of liquid as seen in Figure 3.7(a).
- After some time, Decrease in liquid velocity as a result of cuttings production at bottom. liquid transports the cuttings to the surface thereby lowering its own speed gradually from bottom to top as seen in figure 3.7(b) .
- After some time, an increase in the liquid velocity at the top is observed as gas speed at bottom increases as seen in figure 3.7(c) and 3.7(d).
- At the stop of gas and liquid injection, we see in figure 3.8(a) a rapid reduction in the speed of the liquid at the top, indicating high gas migration to the top. Meaning the speed of the liquid gradually starts to slow down at the top until it becomes zero.
- Figure 3.8(b) shows a negative velocity gradient for the liquid phase close to the top. A fluid which moves in the opposite direction(downward) has a negative velocity and hence a negative acceleration. This means that the liquid begins to decelerate to the bottom.

Cuttings:

- In Figure 3.7(b), cuttings velocity begins to increase at the bottom.
- The velocity of the cuttings is nearly uniform in all the figures. Low velocity profile for the cutting phase indicates a slow cuttings movement in the system.

Gas:

- In figure 3.7(c) and 3.7(d), gas velocity increase is observed from the bottom to the surface.
- At the stop of gas injection, gradual decrease in gas velocity at the bottom as gas diffuses to the top.
- After some time i.e before the end of the test, gas velocity slowly approaches zero as gas now occupies a free region (a region where the gas particles are free to move).

A pictorial view of the liquid-gas-cutting velocity is shown below after time T = 9000 sec.

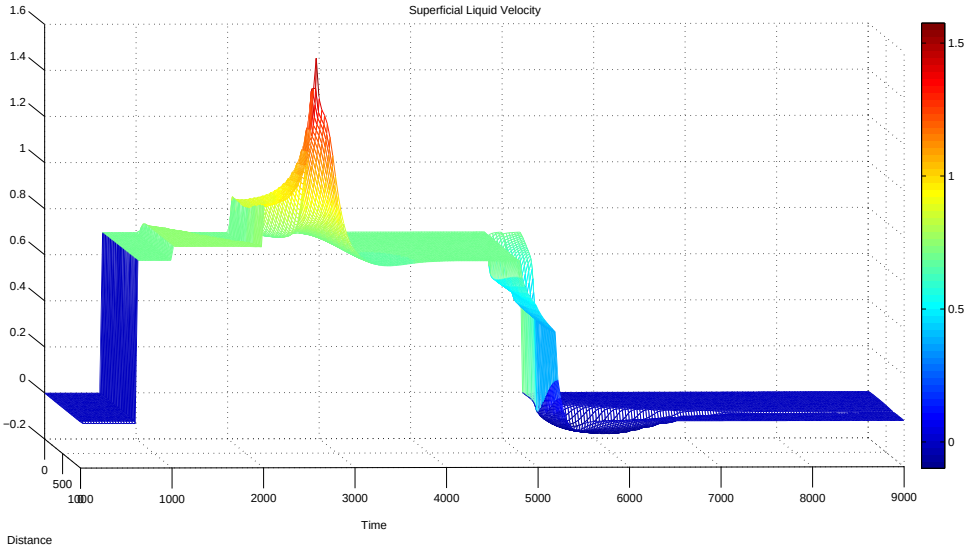

Figure 3.9: liquid superficial velocity

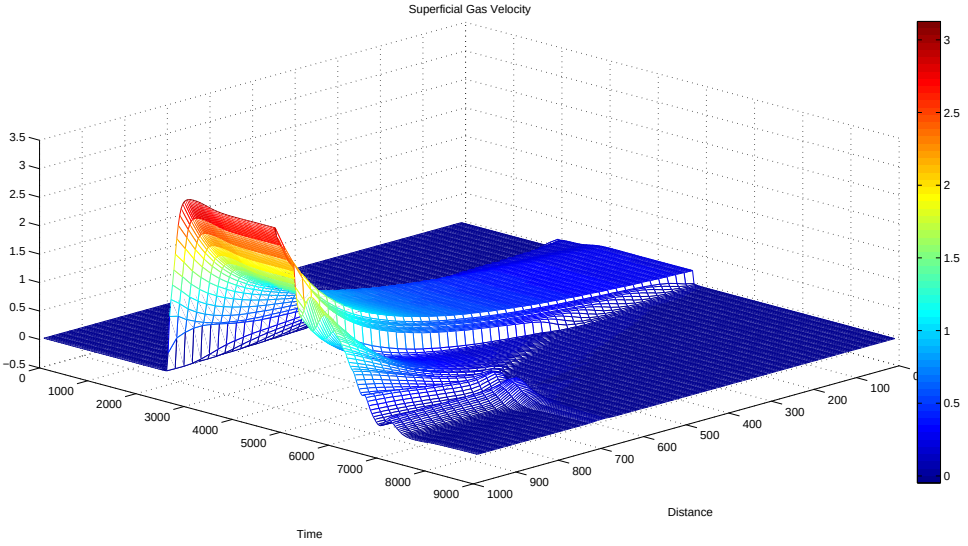

Figure 3.10: gas superficial velocity

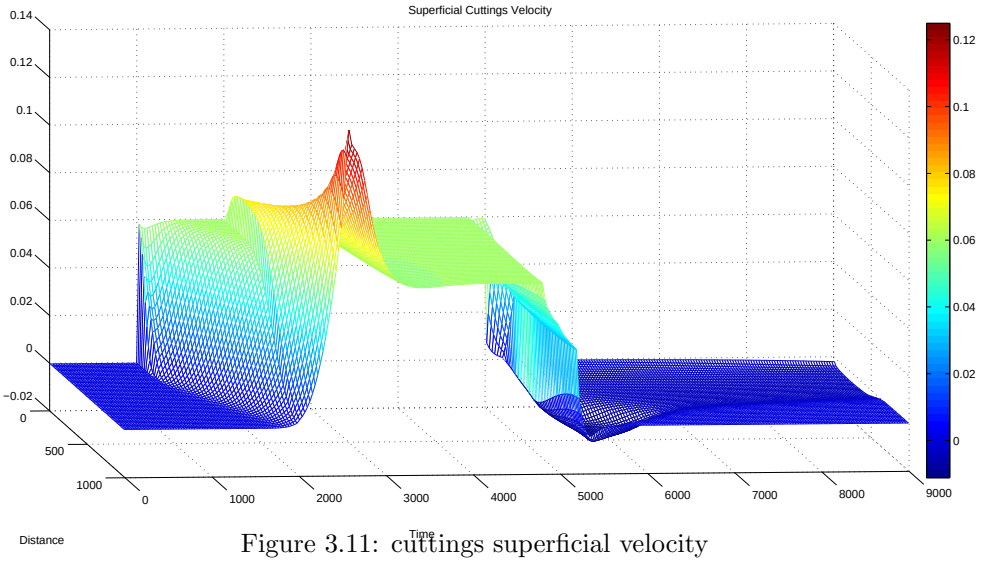

Figure 3.11: cuttings superficial velocity

Pressure(m,n,s):

The plots for the pressure term is shown as a function of the masses of the three phases.

Figures of the pressure graphs were recorded at two different position along the wellbore;
N1 = 2 ; position close to the bottom (indicated by the blue line)
N2 = 49; position close to the top (indicated by the red line)

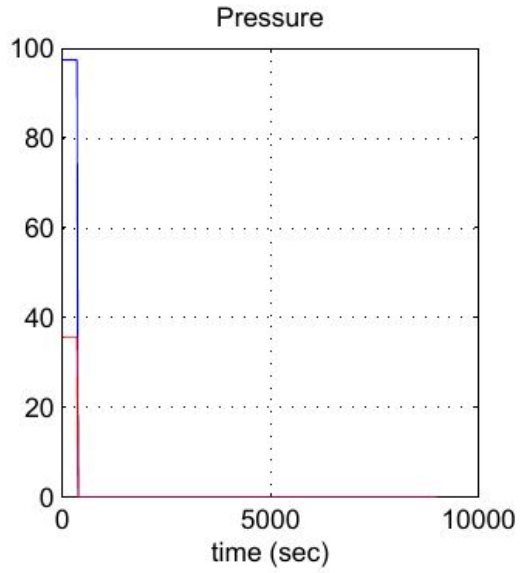

(a) Pressure at initial condition: system is stagnant

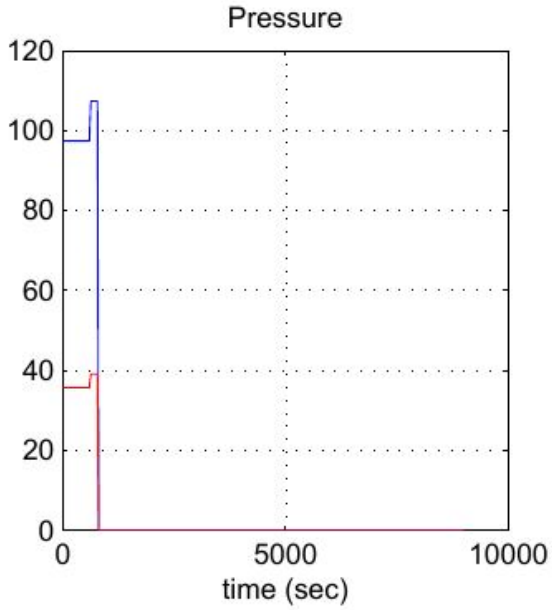

(b) Pressure change due to inflow of liquid at time t = 600 seconds

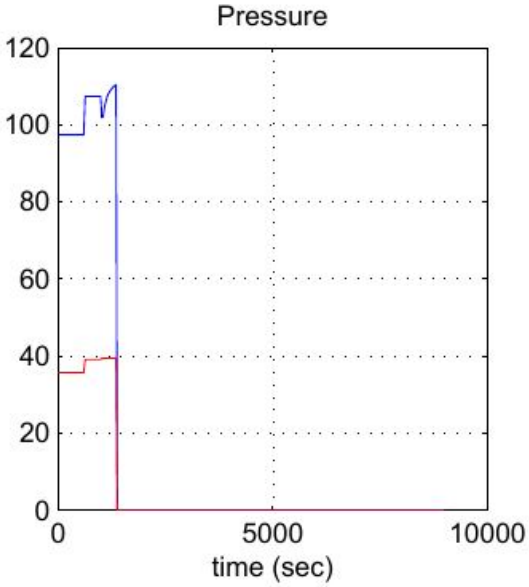

(c) Pressure change due to inflow of cuttings at time t = 1000 seconds

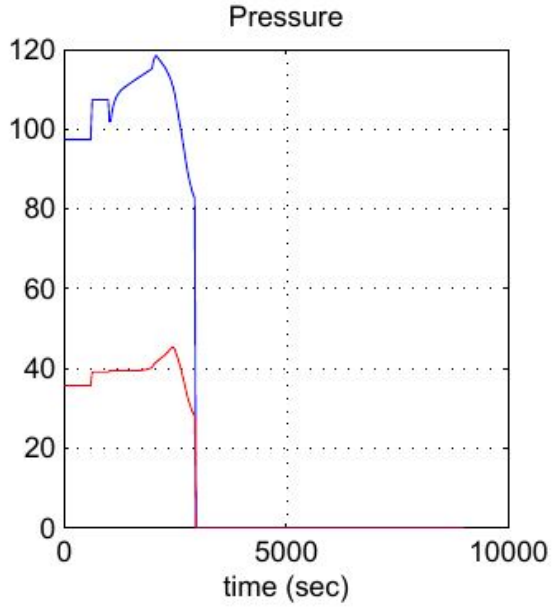

(d) Pressure change due to inflow of gas at time t = 2000 seconds

Figure 3.12: Plots showing pressure variation as a result of inflow of the different phases

- Figure 3.12(a) shows the pressure during the sleeping period of the system (stagnant period).
- At time t = 600 seconds, the inflow of liquid shows a higher increase in pressure at position N1 and a little increase at position N2. we can see this in figure 3.12(b).
- In figure 3.12(c), At time t = 1000 seconds, the inflow of cuttings shows an increase pressure fluctuation at position N1 and no change in pressure at position N2
- Inflow of gas in figure 3.12(d) leads to a decrease in the pressure along the wellbore. This pressure reduction continues until a stable condition is reached. This is shown in Figure 3.13(a)

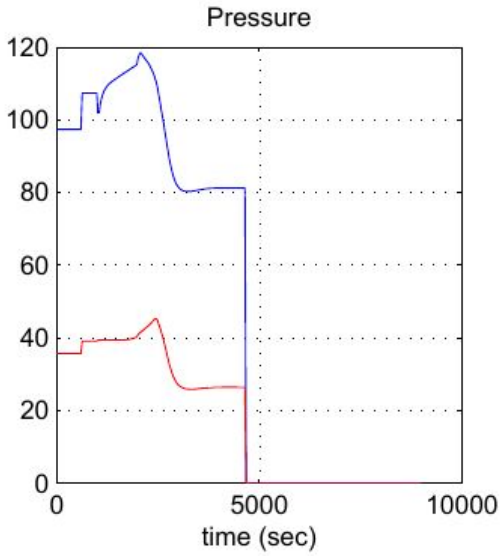

(a) Stable condition reached as we continue to inject gas

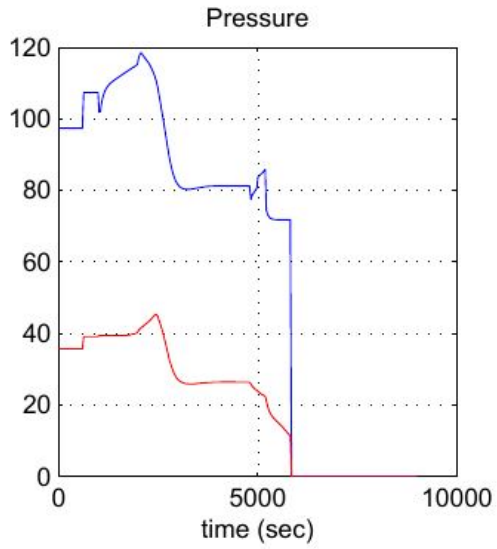

(b) Pressure reduction at the stop of gas and cutting inflow and a stable reading after the stop of liquid injection

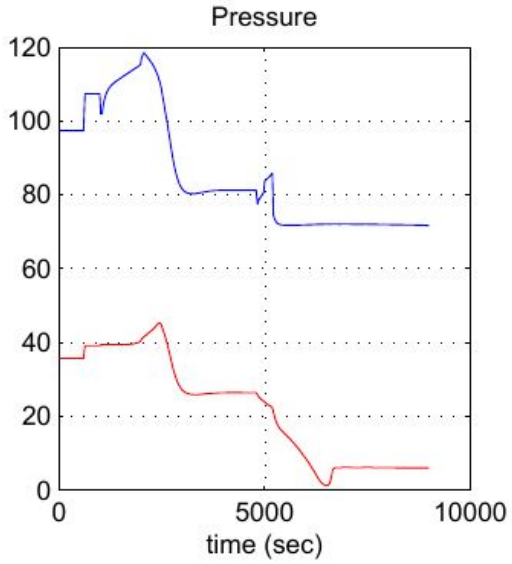

(c) Between $5200 < t < 9000$ sec, uniform pressure condition is reached

Figure 3.13: Pressure plot after the stop of injection of liquid, gas and cutting

- pressure is reduced until it approaches a stable condition. Uniform pressure indicating a steady state situation is reached.
- Stop of the inflow of gas and and cuttings is leads to rapid decrease and immediate increase of pressure at position N1 but a smooth pressure decrease is seen at position N2.
- Stop of the inflow of liquid at t = 5200 seconds results in a decrease in the pressure at the position N1 after which a stable condition is attained but the pressure continues to reduce at position N2 until time t = 6000 seconds where it becomes zero as a result of negative liquid mass rate at position N2. As the liquid mass rate at position N2 starts to approach zero, the pressure at N2 increases to attain a stable uniform condition in Figure 3.13(c)

4 Study Of The Injection Rate And Wall Friction Term

4.1 Model Reformulation

The need for more explanation on major factors affecting the transport of liquid, gas and cutting in a wellbore has led to the creation of this section. In this chapter, focus will be on two transport cases:

- Effect of varying injection rates
- Effect of modifying the frictional term in the momentum equation.

Reformulation of the momentum equation in section two with respect to the use of a new friction term parameter will be carried out and discussed. This will be implemented into the Matlab file to produce result which will show the effect of the new frictional term on the well pressure and a comparison to the former friction term used in section three. Other consideration for the model could include:

- adjustment on the Interphase friction parameter,
- new viscous stress term.
- Inclusion of the interphase pressuree term.i.e phase pressure differenc
- Inclusion of the particle-particle interaction term contribution.

Although these considerations will not be discussed in this work but it is important to point out that adjustment of these terms can be really significant to proper transport in the well.

4.2 Varying of injection rates for the transport system: An example of a base case

Previously in section three, we saw a fixed injection rate used to observe pressure changes as well as void fraction and velocity distribution profiles.

We want to find the solution during the time period [0,T]. How will the void fraction and pressure profile be sensitive to changes in the flow rate $q_L(t)$ at the bottom?

In this section, Injection rates will be varied for the various phases at the bottom of the annulus.

From the literature of [47], liquid and gas Injection rates were tested at 40 GPM and 60 SCFM(373.8 GPM) respectively at an inclination of 30 degrees. Keeping in mind that the standard measurement for volumetric liquid flow is gallon per minute (GPM) and the standard measurement for volumetric gas flow is standard cubic feet per minute (SCFM). The result of the experiment by [47] showed that high gas injection rate increases the volume of foam which is the drilling fluid, leading to a reduction in well pressure and improving overall cuttings transport.

The use of this injection rate might not be so effective in the analysis of a vertical transport system since the settling rate of cuttings at the bottom of a vertical inclination is higher than that at 30 degrees inclination.

Test of various injection rates with reference to the article by [48] on cuttings transport experiment with foam for the case of horizontal and nearly horizontal wellbore inclination can be considered in this section for comparison purpose.

Basic knowledge about varying injection rates is that higher rate of penetration (ROP), increases the cutting volume in the wellbore which requires higher flow rate to clean the hole [49] [Pg.43-44].

4.2.1 Effect of cuttings injection rate on pressure and cuttings deposition

Varying of Cuttings injection rate at $65kgm^3/s$ and $160kgm^3/s$ respectively is shown below. The injection rate for liquid and gas is held constant at $700kgm^3/s$ and $20kgm^3/s$ respectively.

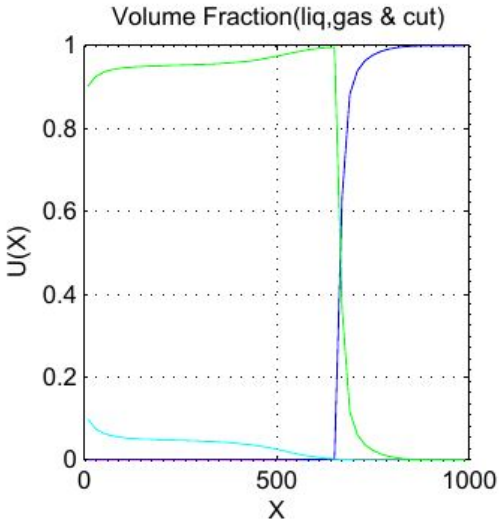

(a) Cuttings injection rate at 65 kgm^3/s after T=9000 secs

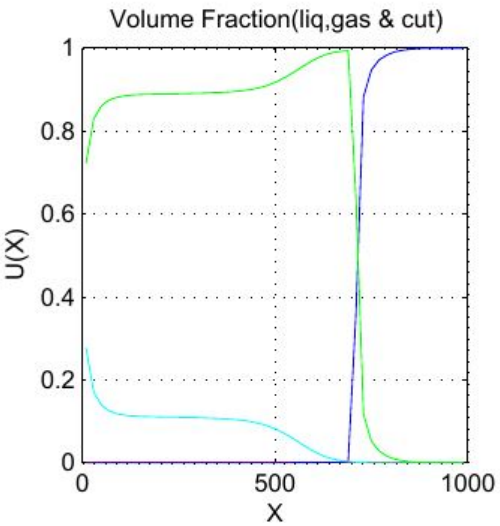

(b) Cuttings injection rate at 160 kgm^3/s after T=9000 secs

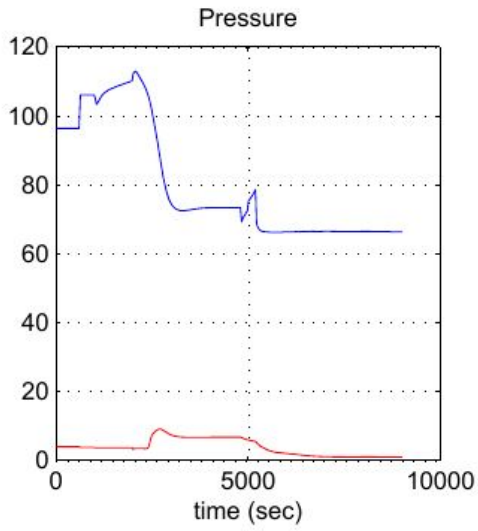

(c) Pressure change at cuttings injection rate of 65 kgm^3/s , after T=9000secs

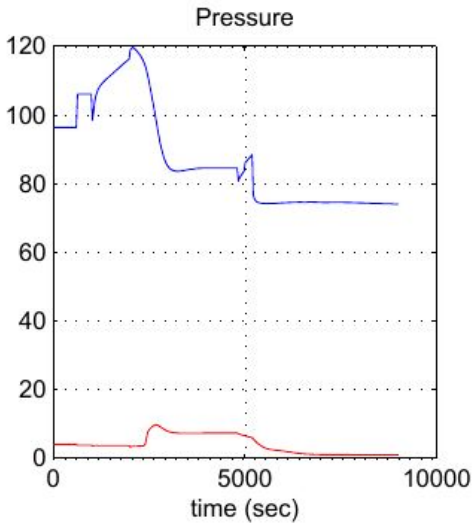

(d) Pressure change at cuttings injection rate of 160 kgm^3/s , after T=9000secs secs

Figure 4.1: The above figures shows cutting injection at 65 kgm^3/s and 160 kgm^3/s respectively.

Observation

Figure 4.1(a) and 4.1(b) show the volume concentration of cuttings after 9000 sec. 4.1(c) and 4.1(d) shows the effect of cuttings injection rate on the bottom hole pressure. Low injection rate, shows Low cuttings deposit at the bottom after stop of well operation and vice versa for high injection rate. High pressure at the bottom between 1000 - 2000 sec due to increased rate of cuttings injection is observed in 4.1(d) as compared

to 4.1(c)

4.2.2 Effect of liquid injection rates on pressure and cuttings removal

As regards to the initial liquid injection rate used in section 3, a look at varying liquid injection rates and its effect on well pressure and the transport of cuttings to the surface. Considering liquid injection rate at 400 kgm^3/s and 1000 kgm^3/s for cuttings injection at 65 kgm^3/s.

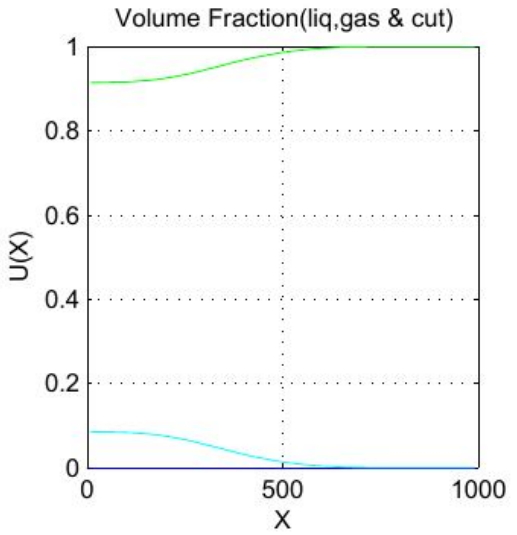

(a) Liquid injection at 400 kgm^3/s versus cuttings injection at 65 kgm^3/s at T=2000 secs just before gas injection

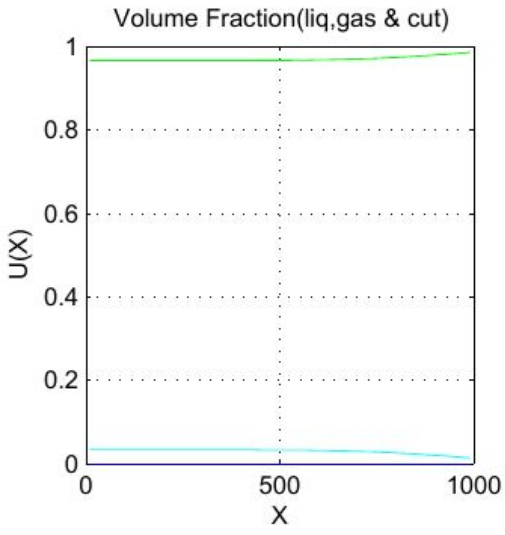

(b) Liquid injection at 1000 kgm^3/s versus cuttings injection at 65 kgm^3/s at T=2000 secs just before gas injection

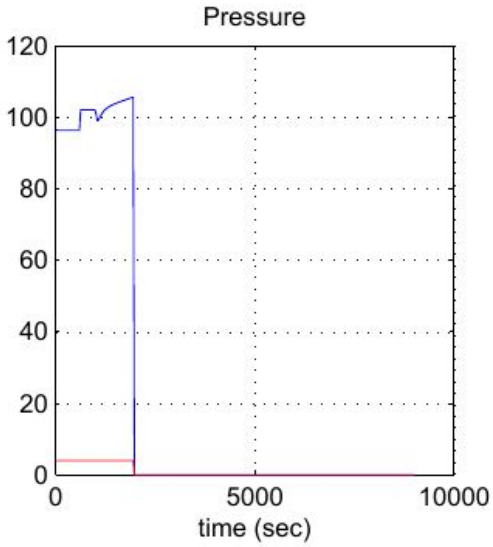

(c) Effect on pressure for Liquid injection at 400 kgm^3/s versus cuttings injection at 65 kgm^3/s at T=2000 secs

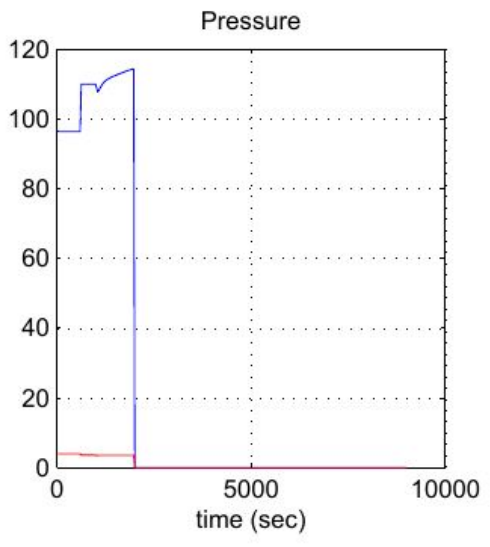

(d) Effect on pressure for Liquid injection at 1000 kgm^3/s versus cuttings injection at 65 kgm^3/s at T=2000 secs

Figure 4.2: The above figures shows a comparison for liquid injection at 400 kgm^3/s and 1000 kgm^3/s with respect to a constant cuttings injection at 65 kgm^3/s.

Observation

From 4.2(a) and 4.2(b), it can be seen that low injection rate of liquid is not sufficient to transport the cuttings to the surface. This is due to the fact that drill cuttings retards fluid flow and increases drilling fluid density. This phenomenon results in low fluid velocity due to the fluid having more cutting weight added to its own weight [50]. This ultimately reduces the ability of the drilling fluid to effectively lift drill cuttings from bottom hole to the surface. But increasing the liquid injection rate in 4.2(b), it can be deduced that it is sufficient lift the cuttings to the surface. The effect of this varying injection rate can also be seen on the pressure profile 4.2(c) and 4.2(d).

4.2.3 Effect of gas injection rate on pressure and cuttings removal

From the literature of [51], required gas injection rates depends mainly on liquid density, liquid-gas interfacial tension, hole size, and depth, and rate of penetration. During cuttings removal, underestimating the minimum required gas injection rate might pose a problem to the drilling operation. Therefore the need for accurate prediction of the required gas injection rate is important. Below will be a test for various injection rate and its effect on cuttings removal and pressure increase.

Previous Analysis shown in section 3 shows gas injection rate at +20 kgm^3/s. Varying this injection rate at 5 kgm^3/s and 100 kgm^3/s for constant cuttings and liquid injection rate at 65 kgm^3/s and 400 kgm^3/s respectively is shown below.

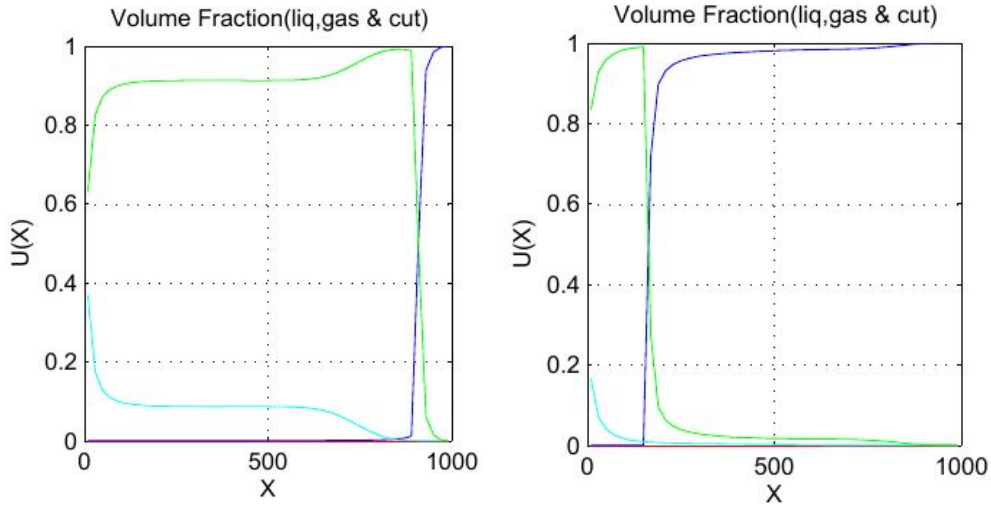

(a) gas injection at 5 kgm^3/s after time T=9000 secs (b) gas injection at 100 kgm^3/s after time T=9000 secs

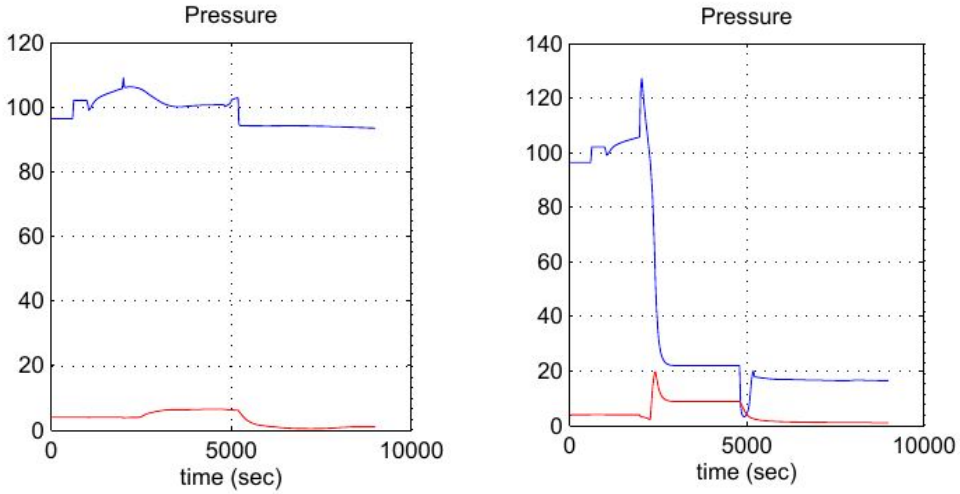

(c) Effect on pressure for gas injection at 5 kgm^3/s after time T=9000 secs (d) Effect on pressure for gas injection at 100 kgm^3/s after time T=9000 secs

Figure 4.3: (a) and (b) shows gas injection at 5 kgm^3/s and 100 kgm^3/s respectively at constant liquid and cuttings injection rate.

.

Observation

Explanation from the resulting graph shows us that cuttings and liquid removal is inefficient at low gas injection rate and highly efficient at high injection rate. The effect on the pressure profile in 4.3(c) and 4.3(d) can be interpreted as the effect of low and high gas injection on pressure. Clearly, low gas injection rate has minimal effect on the pressure profile compared to high gas injection rate which decreases the well pressure. Whenever the fluid level in the hole decreases, the hydrostatic pressure exerted by the fluid also decreases and if the decrease in hydrostatic pressure falls below the formation pore pressure, this will result in a kick(undesirable influx of formation fluid in to the wellbore)[60]

Interpretation:

The following observation and conclusion can be made from the above graphical analysis.

- Higher cutting injection rate will require higher liquid injection rate for efficient removal of cuttings.
- Information for the minimum required gas injection rate is very important for efficient liquid and cutting removal.
- Effect of drill pipe diameter should also be considered for choosing accurate injection rates for liquid, gas and cutting rates.
- Well Pressure profile is highly affected by the rate of gas injection.
- Increasing liquid and cutting injection rate results in increase in well pressure and an increase in gas injection rate results in the decrease in well pressure.

4.3 Modified Frictional Term

As earlier discussed, modeling of the wall friction term of the momentum equation is really important because this is the force that exists between the phases and the wall. The flow of the various phases is hindered by the existence of the frictional force. This force as defined by several literatures is dependent of the flow regime and the wall roughness, therefore leading to the calculation of the Reynolds number. In our earlier base case test, a more simplified frictional term was used which did not put into consideration the nature of flow and the roughness of the annulus wall.

In this section, the main focus will be to implement other recommended frictional term by some authors into the base case and compare results. Also the use of very high fanning friction constant will also be investigated.

First we start up by investigating the reason for the use of a high fanning friction constant in the estimation of the friction term between the various phases and the annulus wall. Already shown in chapter two of model development, the wall shear stress is directly proportional to the flow velocity of the phases where the constant of proportionality is F_I, which is a parameter that describes the drag force between the I-phase and the wall of the annulus. The term F_I will be more or less a complicated function of the volume fractions, flow velocities, densities, and possibly other parameters.

$$\tau_i = F_i u_i \tag{4.1}$$

$$F_i = f \alpha_i \mu_i \tag{4.2}$$

where f = fanning factor.

The fanning factor is a dimensionless quantity that should depend on the roughness of the wall and the flow regime. According to [9], flow in well annulus is usually laminar and thus it is a function of the viscous fluid. It is also important to note that the roughness of the wall annulus is also dependent on the cutting speed (rate of penetration). Low cutting speed results in smoother wall surface [52]. Therefore on this basis, it is likely that our choice of the fanning friction constant in the base case simulation in section three is high since the cuttings production is set at 120 kgm^3/s, implying a high cutting speed (rate of penetration).

If we are to follow the conclusions of [52] on the relation of the friction factor to the roughness of the wall surface, we might just carry out an investigation by first observing varying the fanning friction constant on the pressure profile. Below we take a base case example

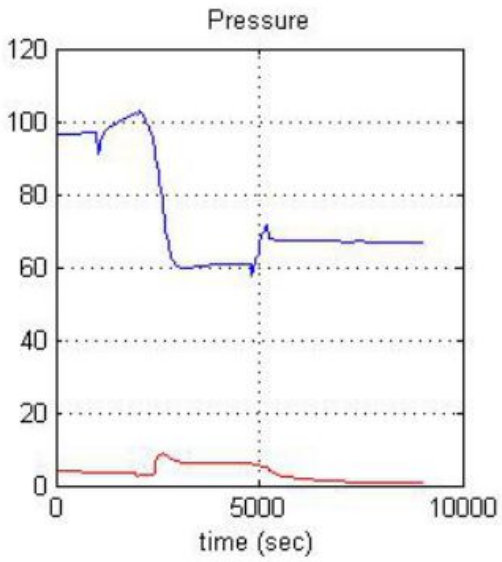

(a) Pressure at Time t = 9000 sec and fann factor = 1000

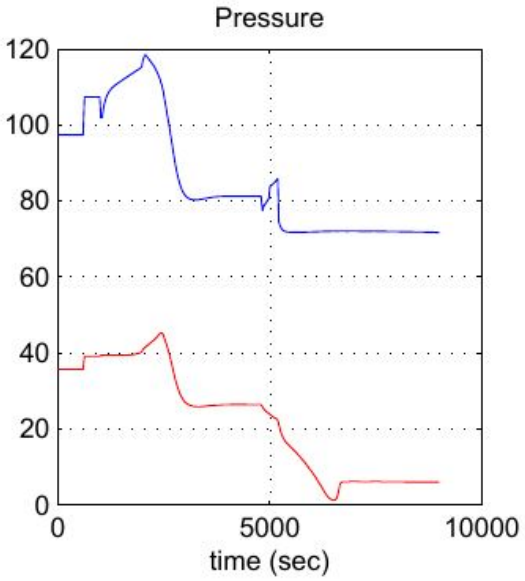

(b) Pressure at Time t = 9000 sec and fann factor = 10000

Figure 4.4: Varying fann factor constant and its effect on the pressure profile. (a) shows a reduced pressure during the inflow of liquid, cuttings and gas at times 600, 1000 and 2000 seconds respectively,stopping the inflow of gas and cuttings at time 5000 seconds show a little increase in the pressure as liquid injection still continues. At time 5200 seconds when liquid inflow is stopped, a little drop in pressure is seen as compared to (b) where a bigger pressure drop is seen.

Interpretation

- Reduced fanning friction constant shows a reduction in pressure profile as a result of the inflow of liquid, cuttings and gas with respect to time. While increasing the fanning friction constant shows an increasing pressure profile(b).
- Pressure measured close to the surface in (a) at time $t > 5200$ seconds goes to 1 bar which actually satisfies the boundary condition at the surface.

- Decreasing the fanning friction constant in (a) shows that pressure close to the surface as indicated with the red line approaches stability much earlier in time than in (b) with increased fanning friction constant.
- Increased friction constant in (b) implies higher wall roughness leading to a increased pressure from inflow of the liquid and cuttings phase, while in (a) a lower wall roughness(smoother wall) leads to reduced pressure from the inflow of the liquid and cuttings phase.

Also we can conclude that varying the cutting inflow rate will only affect the pressure exerted by the flowing cuttings volume either by increasing the pressure at the time of cuttings inflow or reducing the pressure. From this we can also conclude that the phase volume fraction does not really play a major role in shaping the friction term.

Next consideration would be to propose the use of a new friction term by assuming the basics;

- The flow is laminar
- effect of compressibility with respect to phase density

Use of the fanning friction factor formula described in sub section (2.5) for a laminar flow, we can restate the momentum equation for the liquid phase only.

$$\partial_t(mu_l) + \partial_x(mu_l^2) + \alpha_l \partial_x P_l = -f_l - C_1(u_g - u_l) + C_2(u_c - u_l) - mg + \partial_x(\varepsilon_l \partial_x u_l) \tag{4.3}$$

where the friction term is represented as

$$f_l = h_f = F_f \left(\frac{L}{D} \frac{u_l^2}{2g} \right) \tag{4.4}$$

F_f = fanning friction factor is described as;

$$F_f = \frac{16\mu_l}{\rho_l u_l D} \tag{4.5}$$

Inserting this into equation (4.4), we have

$$f_l = \frac{8\mu_l u_l L}{\rho_l g D^2} = 20387.359 \frac{\mu_l}{\rho_l} u_l \tag{4.6}$$

where L=1000 meters is the length of the well, D = 0.2 meters is the diameter of the well, $g = 9.81 m/s^2$ is the gravity term.

Implementing this new friction factor term into the Matlab code, the following graphical figures are shown.

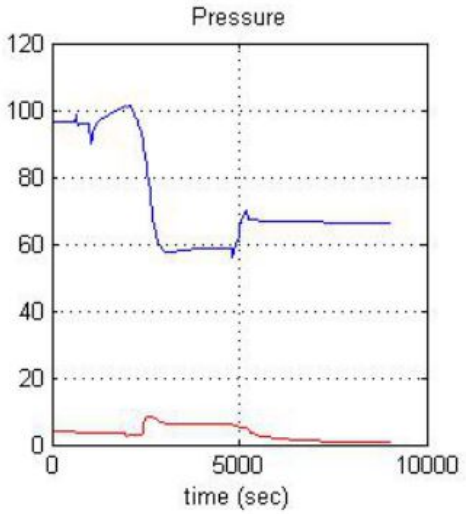

(a) Varying inflow rate at $q_L = 700kgm^3/s$, $q_g = 20kgm^3/s$ and $q_c = 120kgm^3/s$, pressure profile at final time t=9000 sec

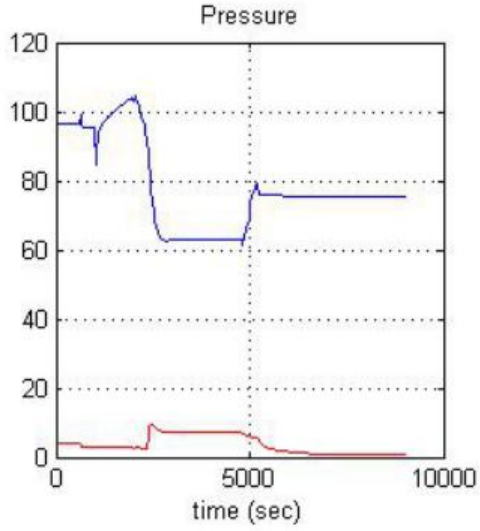

(b) Varying inflow rate at $q_L = 1000kgm^3/s$, $q_g = 25kgm^3/s$ and $q_c = 200kgm^3/s$, pressure profile at final time t=9000 sec

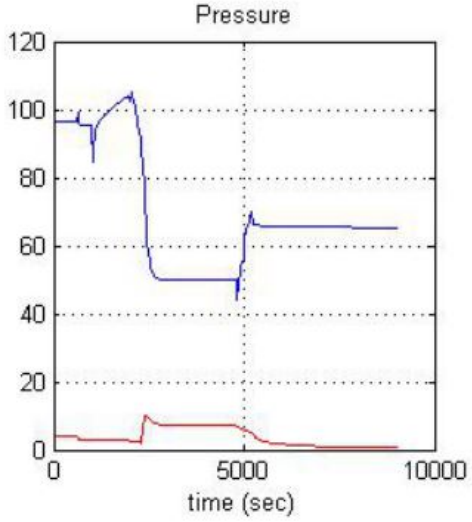

(c) Varying inflow rate at $q_L = 1000kgm^3/s$, $q_g = 35kgm^3/s$ and $q_c = 200kgm^3/s$, pressure profile at final time t=9000 sec

Figure 4.5: Effect of new friction term on well pressure

From The above figures in 4.5(a), (b) and (c), An adjusted friction factor term used which is dependent on the density and viscosity of the flowing phase as compared to the friction term which is dependent on phase volume fraction and viscosity. The effect of phase compressibility for the flow of liquid and gas can be observed in the figures 4.5(a), (b) and (c) above.

The friction force between the wall and the flowing phases affects the well pressure and this is shown in the above figure of (4.5). A conclusion to this is that a well modelled friction factor can ensure a reasonable

control of well pressure.

4.3.1 Comparison between the new and old friction term

The difference between the old friction term and new friction term can be seen below.

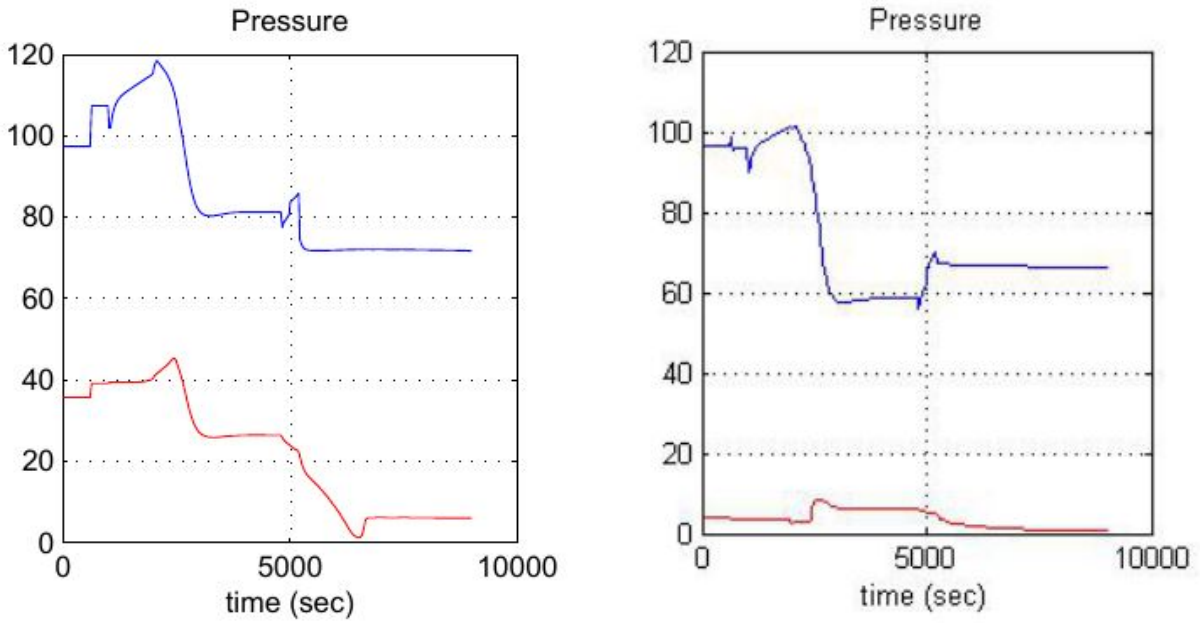

(a) Pressure at Time t = 9000 sec for old friction term

(b) Pressure at Time t = 9000 sec for new friction term

Figure 4.6: Comparison of old and new wall friction term and its effect on the pressure profile.

Interpretation:

The introduction of the new friction term was important to include the effect of the fluid compressibility on the wall friction. From the Figure 4.6(a) and 4.6(b) above, we can deduce that a proper control of the pressure term for flow in laminar well annuli will be to define the wall friction term in such a way that the effect of the fluid compressibility is considered. The reformulation that is done in this section shows a reduced pressure when the new friction term is introduced, as compared to the old friction term. The effect of high liquid, gas and cuttings injection rate on the pressure profile at the surface is minimized.

A recommended choice of the wall friction term for a vertical well annuli will be the fanning friction factor equation.

Conclusion and Recommendation

This thesis describes a transient three phase flow model of liquid, gas and cuttings in a vertical well with specified boundary conditions where we have the injection of fluid and cuttings at the bottom of the well and transported through the well, leading to a production at the surface with strict adherence to the fact that no liquid inflow back into the system from the surface (back drop). This model was introduced by [6] for a two phase flow system. A further adjustment to this model included the addition of the cutting phase. A proper closure model was presented which was in line with the basic assumptions taken.

The importance of the study of a three phase transport system dates back to the industrial challenges in the drilling industry, the effect of the following parameters; choice of the drilling fluid, cuttings size, injection rates, rate of penetration etc. on a proper well cleaning process has lead a lot of researchers to the study of modeling the cuttings transport.

Simplification of this model is the reason why we had several assumptions because the more complex the model is, the more difficult it becomes to analyse. Take for example the viscous term in the momentum equation of (2.14) to (2.16), it can be noticed that not much was said of this term in this work. The difficulty in modelling the viscous term is discussed by several authors [6], [24],[1].

The study of a transient model for cuttings transport using a numeric maths software (Matlab) for simulation purpose is ideal for academic research purpose. The use of the Matlab software for this study was useful in the following ways;

- Vectorized operation is possible.
- The basic data element is the matrix. An integer is considered as a matrix of one row and one column.
- Input of functions and variables can be written easily.
- The graphical output is optimized for interaction. Plotting of data can be easily done.

The Matlab software was used to evaluate the sensitivity of parameters associated with three phase flow in a system. The simulation carried out was based on a real well geometry, fluid and cuttings parameter.

Following the work done in section 2 of this thesis, the discretization of the continuity and momentum equations explicitly is really important since a discrete scheme makes it possible to evaluate parameters using the software tool at present time. It can be seen that the explicit discrete scheme is simple and also can be computed really fast as compared to if it was done implicitly at time t^{k+1}.

The Thesis work is be summarized below;

The work done here shows a less complicated way of determining the velocity of the fluid and cuttings flow in the system. The velocity term at cell j was defined using the central based scheme as seen in equ (2.65). This scheme takes the average of the velocities at the cell interfaces. For a cell J = 1, we can define the velocity term as;

$$u_j = \frac{1}{2}(u_{j+\frac{1}{2}} + u_{j-\frac{1}{2}}) \tag{4.7}$$

$$u_1 = \frac{1}{2}(u_{\frac{3}{2}} + u_{\frac{1}{2}}) \tag{4.8}$$

Where $u_{\frac{1}{2}}$ = velocity at bottom (U_{inlet})

For the velocity at the inlet, the velocity equation can be obtained from equ (3.4) which is written as

$$u_{\frac{1}{2}} = \frac{q_{x=0}}{n_{x=0}A} \tag{4.9}$$

A continuous iteration of this sought using the numeric software will give the velocity profile with respect to the injection rate of the fluid and cuttings. For computing in the numeric software, a superficial velocity term needs to be specified as seen in section 3.

In section 2, the pressure equation as function of the mass of liquid, gas and cuttings respectively was derived and a 3-D graph was shown to highlight the effect of the various parameters on the pressure at all coordinates of the geometry. The effect of the liquid compressibility on the pressure graph was also discussed.

A clear conclusion on this is that the lower the speed of sound for the liquid phase, the more compressible the liquid is which results in reduced pressure as compared to a higher speed of sound for the liquid phase which indicates an incompressible liquid leading to a higher pressure.

A sensitivity analysis is carried out on the simulation result of a base case flow situation with all parameters listed in table 3.1 . The results from the simulation shows the following:

- The rate of fluid and cuttings injection affect the overall transport of these materials to the surface. The effect of the injection rate on the volume fraction, velocity and pressure profile was analysed extensively. A conclusion on this showed that before the injection of gas, at time T = 2000 seconds, The volume of cuttings at the surface is at zero which indicates insufficient transport capacity of the liquid phase.

- It can also be seen that there is a transition to single phase at time T = 9000 seconds. Now this is due to the counter current flow observed at the stop of injection whereby solid particles fall to the bottom instead of being suspended. this effect is attributed to the gravity term. Also with respect to the density property of the fluids, light gas moves upwards and occupies the area towards the surface while heavy liquid is pressed downwards.

- Increasing the injection rate will lead to an increase in the speed of the transported materials. Observation

shows that at the time t = 1000 seconds to 5000 seconds, liquid velocity fluctuation occurs towards the surface. This means that the liquid maintains a constant velocity at the bottom irrespective of the injection of gas and cuttings.

- One of the most important aspect of flow modeling in a well is to learn how to manage the bottom pressure. This pressure needs to be controlled at all times. An increasing injection rates of liquid and cuttings shows a rapid increase in the bottom pressure and an increasing injection of gas shows a decreasing pressure. A major question though is that when is the well pressure stability reached?. The answer to this can be seen in figure (3.13) where at the stop of fluid and cuttings injection, a stabilised pressure is obtained meaning that the effect of counter current is not pronounced on the pressure profile.

- Furthermore, a varying injection rate for cuttings is discussed in section (4). Observation shows that at high cuttings injection rate, single phase transition occurs closer to the surface as compared to reducing the injection of cuttings which shows a single phase transition farther away from the surface. Higher cuttings deposition is also seen at the bottom, at the end of the operation, T = 9000 seconds for increasing injection rate.

- The discussion on the effect of varying the liquid injection rate shows that increased liquid injection is necessary for effective transport of the cuttings but the resulting effect is an increased well pressure at the bottom.

- Also fascinating is the effect of the gas injection rate on the various parameters. At low gas injection, a good cuttings suspension is seen at the stop of operation. The transition to single phase is so close to the surface and the effect on the pressure profile is very minimal. But an increase in the injection rate shows an effective cuttings transport implying that more suspending fluid were transported to the surface and the transition to single phase occurs really close to the bottom. The effect of this on the pressure profile is not really an expected result because we would like to keep the well pressure within certain expected range.

In the last part of section four, Model reformulation involving the replacement of the friction factor with a more well defined term which takes into account the type of flow regime is carried out. The initial idea was to propose a new friction term which considers wall roughness as well as the flow regime but due to the difficulty of finding an experimental research work which has dealt with this issue, I had to propose the wall friction term based on a simple assumption for laminar flow.

The difference between the old friction term and new friction term as seen in Figure 4.6 shows that the new friction term gives a better result for well pressure control. This new friction term is made on the assumption that the flow is laminar. For a more turbulent flow, this might not be appropriate to use.

The importance of this information to a drilling firm is in line with the challenges of the use of proper models to predict well pressure gradients. The effect of improper prediction of the well pressure can be read in several literatures.

One recent technology by a drilling firm, Reelwell, shows a huge success with effective cuttings transport in a pressurised mud cap drilling system and constant well pressure for managed pressure drilling system by developing a dual drill pipe, that has two flow channels, one for the flow of drilling fluid into the well down to the bit and the other for the return flow of fluid from the bottom of the well back to the surface. This technology which was developed in Norway and tested in the middle east might just be a breakthrough to the drilling industry challenges.

Recommendations for further research

The complexity of the viscous term in the momentum equation is a disturbing factor, hence proper modeling of this term which will consider both laminar and turbulent flow regimes is required. In general, this work was carried out for a vertical well geometry. Future research should involve modeling of deviated and horizontal well geometries with proper boundary conditions and closure laws.

From the simulation done in this work, it can be seen that for an effective transport of cuttings, higher liquid flow rate is required, leading to high well pressure gradient. Future work on this should focus on developing models which would require lower liquid flow rate for effective cuttings transport.

Appendix

List of Figures

1.1 Figure showing the flow regime of the Fluid Solid transport in a vertical pipe Adapted from [20] 5
1.2 Figure showing the flow regime of the Liquid Gas transport in a vertical pipe adapted from [45] 6
1.3 Forces acting on a particle settling through a fluid. [53] 8
1.4 Schematic of solid particle transport process in a vertical and horizontal / deviated well [54] . . 8
1.5 Well geometry of various inclinations.[49] 9
2.1 3-D graph showing pressure as a function of m,n and s at liquid sound velocity $a_L = 1000$ m/s. 24
2.2 3-D graph showing pressure as a function of m,n and s at liquid sound velocity $a_L = 1500$ m/s. 25
2.3 Point mass m at a distance r from the axis of rotation 28
2.4 Diagram of the Fanning friction factor for pipe flow 33
2.5 Initial state for mass of the various phases 38
2.6 Initial state for the fluid velocity of (liquid, Gas and Cuttings) 39
3.1 Inflow rate of the three phases 43
3.2 Variation in Volume fractions of all three phases 44
3.3 Variation in Volume fractions of all three phases 45
3.4 Observation of the behaviour of the curves at the stop of injection and also the transition to single phase 46
3.5 Figure showing cutting particles occupying lower side of the wellbore. 47
3.6 Volume fractions 48
3.7 Figure showing the Velocity Profile of the three different phases 49
3.8 Velocity profile after the stop of injection 50
3.9 liquid superficial velocity 51
3.10 gas superficial velocity 52
3.11 cuttings superficial velocity 52
3.12 Plots showing pressure variation as a result of inflow of the different phases 53
3.13 Pressure plot after the stop of injection of liquid, gas and cutting 54
4.1 The above figures shows cutting injection at 65 kgm^3/s and 160 kgm^3/s respectively. 58
4.2 The above figures shows a comparison for liquid injection at 400 kgm^3/s and 1000 kgm^3/s with respect to a constant cuttings injection at 65 kgm^3/s. 59
4.3 (a) and (b) shows gas injection at 5 kgm^3/s and 100 kgm^3/s respectively at constant liquid and cuttings injection rate. 61

4.4 Varying fann factor constant and its effect on the pressure profile. (a) shows a reduced pressure during the inflow of liquid, cuttings and gas at times 600, 1000 and 2000 seconds respectively,stopping the inflow of gas and cuttings at time 5000 seconds show a little increase in the pressure as liquid injection still continues. At time 5200 seconds when liquid inflow is stopped, a little drop in pressure is seen as compared to (b) where a bigger pressure drop is seen. 63
4.5 Effect of new friction term on well pressure 65
4.6 Comparison of old and new wall friction term and its effect on the pressure profile. 66

List of Tables

1.1 comparison between the two fluid approach and the drift flux approach. see [26] 3
3.1 Model parameters that have been used for the test case 41

References

References

Textbooks:

[1] Kleinstreuer,C.(2003), "Two-phase flow: Theory and applications",Taylor & Francis Books, Inc, New York, NY.

[2] Govier W. George, Aziz Khalid (2008),"The flow of complex mixtures in pipes", Society of petroleum engineers, TX USA.

[3] Crowe, C., Sommerfeld, M., and Tsuji,Y. (1998) "Multiphase flows with droplets and particles," CRC Press, Boca Raton, FL.

[4] Fan,L. S., and Zhu, C. (1998) "Principle of Gas-Solid Flows," Cambridge University press, New York, NY.

[5] Wallis B. Graham (1969) "one dimensional two phase flow" McGraw-Hill Inc, USA.

[6] Prosperetti Andrea, Grétar Tryggvason (2007) "computational methods for multiphase flow" cambridge university press, United kingdom UK.

[7] Guan Heng Yeoh, Jiyuan Tu (2010) "Computational Techniques for Multiphase Flows" Elsevier Ltd, Oxford UK.

[8] Anderson D.A.,Sundaresan .S., and R. Jackson (1995) "Instabilities and the formation of bubbles in fluidized beds". Journal of Fluid Mech., 303: 327-366, Cambridge University Press USA.

[9] Ryen Caenn, Henry C. H. Darley, George Robert Gray (2011) "Composition and Properties of Drilling and Completion Fluids" Gulf professional publishing 225 Wyman street, Waltham, MA 02451, USA .

Related works

[10] R. Alfredo Sanchez, J.J. Azar, A.A. Bassal and A.L. Martins, (1999) " Effect of Drillpipe Rotation on Hole Cleaning During Directional-Well Drilling" SPE Journal, Vol. 4, No. 2,.

[11] C.T. Crowe (2000)"On models for turbulence modulation in fluid particle flows" International Journal of Multiphase Flow 26 719-727.

[12] H.Shi, J.A Holmes, L.J Durlofsky, K. Aziz, L.R Diaz, B. Alkaya, G.Oddie (2005) "drift flux modelling of two phase flow in wellbores". SPE Journal.

[13] Y. LI, E. KURU (2005) "Numerical Modelling of Cuttings Transport With Foam in Vertical Wells", page.33, Journal of Canadian Petroleum Technology, Vol. 44, No. 3

[14] Bendiksen, K., Maines, D., Moe R.,& Nuland S.(1991) "The dynamic two fluid model OLGA: Theory and application". SPE production Engineering 6(2).pg 171-180.

[15] Issa R.I., Kempf M.H.W. (2003) "simulation of slug flow in horizontal and nearly horizontal pipes with the two fluid model" International journal of Multiphase flow vol.29,69-95.

[16] Hand, N.P.(1991) "Gas-liquid co-current flow in a horizontal pipe". PhD Thesis, Queen's University Belfast.

[17] Hasan Rashid A.,Kablr Shah C.(1988) "A Study of Multiphase Flow Behavior in Vertical Wells" SPE Production Engineering.

[18] Aziz, K., Govier, G.W., and Fogarasi, M. (1972) "Pressure Drop in Wells Producing Oil and Gas," 1. Cdn. Pet. Tech. 38-47.

[19] Chierici, G.L., Ciucci, G.M., and Sclocchi, G.(1974) "Two-Phase Vertical Flow in Oil Wells-Prediction of Pressure Drop," lPT 927-38; Trans., AIME, 257.

[20] Grace J.R (1986) "Contacting modes and behaviour classification of gas-solid and other two-phase suspensions," Can. J. of Chem. Eng.,64,353-363.

[21] Stokes, G. G (1850) "On the Effect of the Internal Friction of Fluids on the Motion of Pendulums" Transactions of the Cambridge Philosophical Society, Vol. 9, page 8.

[22] Holman, J. P. (2002). "Heat Transfer". McGraw-Hill Inc. p. 207.

[23] Manuel. F. Jerez-Carrizales, J. E. Jaramillo and D. A. Fuentes (2014) "Simulation of the two phase flow in a wellbore using two-fluid model" Universidad Industrial de Santander, Bucaramanga, Colombia.

[24] Ishii, Mamoru and Hibiki, Takashi (2011) "Thermo-fluid dynamics of two-phase flow" Springer New York.

[25] Jorge A. Pita, Sankaran Sundaresan (1991) "Gas-solid flow in vertical tubes" AIChE Journal vol. 37, No. 7.

[26] P.Spesivtsev, K. Sinkov & A.Osiptsov (2013) "Comparison of drift-flux and multi-fluid approachesto modeling of multiphase flow in oil and gas wells" WIT Press vol 79.

[27] Tobias Strömgren (2008) "Modelling of turbulent gas-particle flow" Technical report, Universitets service US-AB, Stockholm.

[28] Sommerfeld, M.(2000) "Theoretical and experimental modelling of particulate flows" Lecture Series, von Karman Institute of Fluid Dynamics part I and II, 1–63.

[29] Marion W. Vance, Kyle D. Squires and Olivier Simonin (2006) "Properties of the particle velocity field in gas-solid turbulent channel flow". ICMF'04 Paper No.530.

[30] Yiming Li and J. B. McLaughlin, K. Kontomaris, L. Portela (2001) "Numerical simulation of particle-laden turbulent channel flow" American Institute of Physics.

[31] Osiptsova A.A, Starostina A.B. , and Krasnopolsky B.I.(2012) "Development of a multi-fluid model for multiphase flows in oil and gas wells" 9th EFMC , Italy, Rome.

[32] Bestion, D. (1990) "The physical closure laws in the CATHARE code". Nuclear Engineering and Design, volume 124, no. 3: pages 229–245.

[33] Ndjinga Michaël (2007) "Influence of interfacial pressure on the hyperbolicity of the two-fluid model" C. R. Acad. Sci. Paris, Ser. I 344 407–412.

[34] Munkejord Svend Tollak (2006) "Analysis of the two-fluid model and the drift-flux model for numerical calculation of two-phase flow" Doctoral Thesis at NTNU, 2005:219 Trondheim.

[35] Flåtten, T.(2003) "Hybrid flux splitting schemes for numerical resolution of two phase flows". Doctoral thesis, Norwegian University of Science and Technology, Department of Energy and Process Engineering, Trondheim, ISBN 8247156709.

[36] Goldschmidt M.J.V, Beetstra R., Kuipers J.A.M.(2004) "Hydrodynamic modelling of dense gas-fluidised beds: comparison and validation of 3D discrete particle and continuum models" Powder Technology 142, 23 – 47.

[37] Wen Y.C., Yu Y.H. (1966) "Mechanics of fluidization", Chem. Eng. Prog.Symp. Ser. 62, 100 – 111.

[38] Edwards J. R. (1997) "A low-diffusion flux-splitting scheme for Navier–Stokes calculations", Computational Fluids 26, 635.

[39] Evje Steinar and Kjell K. Fjelde (2002) "Hybrid Flux-Splitting Schemes for a Two-Phase Flow Model" Journal of Computational Physics 175, 674–701.

[40] McGovern Jim (2011) "Technical Note: Friction Factor Diagrams for Pipe Flow" Dublin Institute of Technology.

[41] Faith A. Morrison (2013) "Data Correlation for Friction Factor in Smooth Pipes" Department of Chemical Engineering, Michigan Technological University, Houghton, MI 49931.

[42] Taitel,Y;Duckler,A.E,(1976) "A model for predicting flowregime transitions in horizontal and near horizontal gas-liquid flow, AIChE Journal , 22, pp. 47-55.

[43] Jukka Kiijärvi (2011) "Darcy Friction Factor Formulae in Turbulent Pipe Flow" Lunowa Fluid Mechanics Paper 110727.

[44] Yuan, Z. and Michaelides, E (1992) " Turbulence modulation in particulate flows - A theoretical approach" Int. J. Multiph. Flow, 18: 779-785.

[45] Weisman, J.(1983) "Two-phase flow patterns". Chapter 15 in Handbook of Fluids in Motion (eds: N.P. Cheremisinoff and R. Gupta), Ann Arbor Science Publ., 409-425.

[46] Sinclair J.L and., Jackson R.(1989) "Gas-particle flow in a vertical pipe with particle-particle interactions", AIChE Journal 35 (9), 1473-1486.

[47] Osunde.O. and Kuru.E.(2008) "Numerical modelling of cuttings transport with foam in inclined wells" Open fuels and energy science journal,1, 19-33.

[48] Stefan Miska- Principal Investigator (2003-2004), Troy Reed- Principal Investigator (2000-2003), Ergun Kuru- Principal Investigator (1999-2000), Nicholas Takach- Co-Principal Investigator, Kaveh Ashenayi- Co-Principal Investigator, Ramadan Ahmed- Research Associate, Mengjiao Yu- Research Associate, Mark Pickell- Project Engineer, Len Volk- Research Associate, Mike Volk- Project Manager, Barkim Demirdal Affonso Lourenco Evren Ozbayoglu Paco Vieira Lei Zhou Zhu Chen Aimee Washington Crystal Redden Sameer Nene Jagruthi Godugu Ameen Al-hosani. (2004)"Advanced Cuttings Transport Study" The University of Tulsa 600 South College Avenue Tulsa, Oklahoma 74104 USA.

[49] Girmaa Jiimaa (2013)"Cutting transport models and parametric studies in vertical and deviated wells" Master Thesis, M.Sc. in Petroleum Technology, University of Stavanger.

[50] Fadairo .A. Samson, Ako churchill, Nwaokete Emmanuel and Falode olugbenga (2012) "Improved model for predicting the required minimum gas injection rate for removal of cutting during underbalanced drilling" Society of petroleum engineers SPE 160846.

[51] M.Tabatabei, A.Ghalambor and B.Guo.(2008) "the minium required air/gas injection rate for liquid removal in air/gas drilling" Society of petroleum engineers SPE 116135.

[52] A. Munia Raj, Sushil Lal Das and K. Palanikumarr (2013)"Influence of Drill Geometry on Surface Roughness in Drilling of Al/SiC/Gr Hybrid Metal Matrix Composite"Indian Journal of Science and Technology — Print ISSN: 0974-6846 — Online ISSN: 0974-5645.

[53] Nikos Drakos (1993) "mass transport processes" Computer Based Learning Unit, University of Leeds .

[54] Doguhan Yilmaz (2007) "Discrete phase simulations of drilled cuttings transport in highly deviated wells" M.Sc. Thesis, Graduate Faculty of the Louisiana State University and Agricultural and Mechanical College, USA.

Web Page Sources

[55] Petroblogger (2013) "flow regimes in horizontal and vertical pipes", http://www.ingenieriadepetroleo.com/2013/01/flow-regimes-in-horizontal-and-vertical-pipes.html, viewed 10th March 2015.

[56] Wikipedia "Reynolds number" http://en.wikipedia.org/wiki/Reynolds number, viewed 3rd February 2015

[57] Neutrium (2012)"fluid flow/pressure loss in pipe" https://neutrium.net/fluid flow/pressure-loss-in-pipe/.viewed 13th March 2015

[58] Andy and Steve Shipway (2008) "calculation tool for friction factor", http://www.calctool.org/CALC/eng/civil/friction factor. viewed 10th May 2015

[59] Engineering tool box "Colebrook equation" http://www.engineeringtoolbox.com/.viewed 10th May 2015

[60] Wikipedia "well control" http://en.wikipedia.org/wiki/Well control

. viewed 5th January 2015